



Can the Responses of Photosynthesis and Stomatal Conductance to Water and Nitrogen Stress Combinations Be Modeled Using a Single Set of Parameters?

Ningyi Zhang^{1,2,3†}, Gang Li^{1†}, Shanxiang Yu^{1†}, Dongsheng An¹, Qian Sun¹, Weihong Luo^{1*} and Xinyou Yin^{2*}

¹ College of Agriculture, Nanjing Agricultural University, Nanjing, China, ² Center for Crop Systems Analysis, Department of Plant Sciences, Wageningen University & Research, Wageningen, Netherlands, ³ Horticulture and Product Physiology Group, Department of Plant Sciences, Wageningen University & Research Centre, Wageningen, Netherlands

OPEN ACCESS

Edited by:

Gernot Bodner,
University of Natural Resources and
Life Sciences, Austria

Reviewed by:

Georgios Liakopoulos,
Agricultural University of Athens,
Greece
Daniel Tholen,
University of Natural Resources and
Life Sciences, Austria

*Correspondence:

Weihong Luo
lwh@njau.edu.cn
Xinyou Yin
xinyou.yin@wur.nl

[†]These authors have contributed
equally to this work.

Specialty section:

This article was submitted to
Crop Science and Horticulture,
a section of the journal
Frontiers in Plant Science

Received: 28 September 2016

Accepted: 24 February 2017

Published: 28 March 2017

Citation:

Zhang N, Li G, Yu S, An D, Sun Q,
Luo W and Yin X (2017) Can the
Responses of Photosynthesis and
Stomatal Conductance to Water and
Nitrogen Stress Combinations Be
Modeled Using a Single Set of
Parameters? *Front. Plant Sci.* 8:328.
doi: 10.3389/fpls.2017.00328

Accurately predicting photosynthesis in response to water and nitrogen stress is the first step toward predicting crop growth, yield and many quality traits under fluctuating environmental conditions. While mechanistic models are capable of predicting photosynthesis under fluctuating environmental conditions, simplifying the parameterization procedure is important toward a wide range of model applications. In this study, the biochemical photosynthesis model of Farquhar, von Caemmerer and Berry (the FvCB model) and the stomatal conductance model of Ball, Woodrow and Berry which was revised by Leuning and Yin (the BWB-Leuning-Yin model) were parameterized for *Lilium* (*L. auratum* × *speciosum* “Sorbonne”) grown under different water and nitrogen conditions. Linear relationships were found between biochemical parameters of the FvCB model and leaf nitrogen content per unit leaf area (N_a), and between mesophyll conductance and N_a under different water and nitrogen conditions. By incorporating these N_a -dependent linear relationships, the FvCB model was able to predict the net photosynthetic rate (A_n) in response to all water and nitrogen conditions. In contrast, stomatal conductance (g_s) can be accurately predicted if parameters in the BWB-Leuning-Yin model were adjusted specifically to water conditions; otherwise g_s was underestimated by 9% under well-watered conditions and was overestimated by 13% under water-deficit conditions. However, the 13% overestimation of g_s under water-deficit conditions led to only 9% overestimation of A_n by the coupled FvCB and BWB-Leuning-Yin model whereas the 9% underestimation of g_s under well-watered conditions affected little the prediction of A_n . Our results indicate that to accurately predict A_n and g_s under different water and nitrogen conditions, only a few parameters in the BWB-Leuning-Yin model need to be adjusted according to water conditions whereas all other parameters are either conservative or can be adjusted according to their linear relationships with N_a . Our study exemplifies a simplified procedure of parameterizing the coupled FvCB and g_s model that is widely used for various modeling purposes.

Keywords: mesophyll conductance, model, nitrogen, photosynthesis, stomatal conductance, water

INTRODUCTION

In the past decades, many crop models have been developed for predicting yield in response to changing environments. Some studies evaluated the performance of different crop models under different growth conditions such as different temperature, water supply and soil fertility (Jamieson et al., 1998; Adam et al., 2011; Palosuo et al., 2011). Surprisingly, when testing these models under a large land scale or long time span, the yield predictions in most models turned out to be an artifact of the balance between incorrect predictions of assimilation and leaf area index (Jamieson et al., 1998) or between biomass production and harvest index (Palosuo et al., 2011). The radiation-use efficiency approach that was taken in many crop models may over-simplify underlying processes and a more detailed approach, based on quantitative functional relationships for underlying processes, is needed in order to capture the effects of high temperature and high radiation intensities on crop growth under changing environments (Challinor et al., 2009; Adam et al., 2011). While detailed models usually require more effort in terms of model parameterization, some parameters and functional relationships are found to change very little (i.e., are conservative) among crop types (von Caemmerer et al., 2009) and environmental conditions (Yin, 2013). Therefore, it is important to test the conservative level of commonly used functional relationships, so as to balance between the level of detail in these models and the efforts needed for model parameterization.

Photosynthesis is the primary physiological process that drives crop growth and productivity and influences many plant quality traits, and is strongly affected by environmental factors. Accurately predicting photosynthesis is the first step toward predicting crop growth, yield and quality in response to environmental changes. Water and nitrogen variations frequently occur in crop fields. The effects of water and nitrogen on photosynthesis have been extensively and separately studied (Grassi et al., 2002; Xu and Baldocchi, 2003; Gu et al., 2012). The combined effect of water and nitrogen on photosynthesis, however, has received less attention.

Previous modeling studies have shown that the use of empirical factors to capture the effect of stresses, does not model photosynthesis reliably in many cases (Jamieson et al., 1998). The effects of environmental factors on leaf photosynthesis can be best investigated by use of the biochemical model of Farquhar, von Caemmerer and Berry (the FvCB model hereafter) (Farquhar et al., 1980) combined with diffusion models. The FvCB model has been widely used to describe photosynthesis in response to multiple environmental changes (Harley et al., 1992; Grassi et al., 2002; Xu and Baldocchi, 2003; Monti, 2006; Qian et al., 2012). The model describes photosynthesis as the minimum of the Rubisco-limited rate and the electron transport-limited rate. Major parameters in this model are the maximum Rubisco carboxylation rate (V_{cmax} , definitions of all model variables hereafter are listed in **Table 1**), the maximum electron transport rate (J_{max}) and the mitochondrial day respiration (R_d). These biochemical parameters have been found to be linearly correlated with leaf nitrogen content per unit leaf area (N_a) under environmental changes such as various nitrogen supply (Grassi

et al., 2002; Yin et al., 2009) and elevated CO_2 (Harley et al., 1992; Yin, 2013), as well as seasonal changes (Zhu et al., 2011). However, whether or not the linear relationships between these biochemical parameters and N_a exist under drought is debatable, mainly due to inconsistent effect of drought on N_a (Díaz-Espejo et al., 2006; Damour et al., 2008, 2009).

The FvCB model itself requires the CO_2 concentration in the chloroplast (C_c) as an input variable. To this end, estimating stomatal conductance (g_s) and mesophyll conductance (g_m) is necessary to enable the FvCB model to predict photosynthesis using the atmospheric CO_2 level (C_a) as input. The stomatal conductance model of Ball et al. (1987) (the BWB-type model hereafter), as one of the most commonly used models of g_s , is often coupled with the FvCB model (Harley et al., 1992; Kosugi et al., 2003). In the BWB-type model, g_s responds to net photosynthetic rate, relative humidity and CO_2 concentration at the leaf surface. Although it is phenomenological, the BWB-type model is widely used to model g_s at leaf level (e.g., Leuning, 1995) and is the most feasible yet biologically robust tool for extrapolating g_s at the field or forest stand level (Misson et al., 2002; Alton et al., 2007). The original BWB-type model does not capture stomatal responses to soil water status, thus some efforts were made toward modifying the BWB-type model to predict g_s under drought. Either the slope used in the BWB-type model (describing the response of g_s to photosynthetic rate, relative humidity or vapor pressure deficit (VPD) and CO_2 concentration) (Tuzet et al., 2003; Maseyk et al., 2008; Héroult et al., 2013) or the residual stomatal conductance (the value of g_s when irradiance approaches to zero) (Misson et al., 2004) was reported to decrease under drought, and was related to soil moisture or leaf water potential (Baldocchi, 1997; Wang and Leuning, 1998; Misson et al., 2004; Keenan et al., 2010; Egea et al., 2011; Li et al., 2012; Zhou et al., 2013; Müller et al., 2014). In another study, however, neither of these two parameters was affected by drought (Xu and Baldocchi, 2003). So far, there is no consensus as to how to adjust the BWB-type model parameters to properly model g_s under drought. Moreover, there are very few studies that investigated the responses of these parameters to nitrogen supply and to the combination of water and nitrogen supply.

g_m has been considered as infinite in most early studies, in which intercellular CO_2 concentration (C_i) was used to substitute C_c in the FvCB model (Harley et al., 1992; Kosugi et al., 2003). However, this assumption has later been proved not true since C_c is lower than C_i (Warren, 2004). Ignoring g_m leads to the underestimation of V_{cmax} , especially under stress conditions such as drought (Monti, 2006). g_m has been found to decrease under water-deficit conditions and low nitrogen availability in many previous studies (reviewed in Flexas et al., 2008). There have been only a few attempts to incorporate the effect of drought on g_m in the photosynthesis model by using a dependence of g_m on g_s (Cai et al., 2008) based on the observation of a close correlation between g_s and g_m in response to water-deficit conditions (Flexas et al., 2002; Warren, 2008; Perez-Martin et al., 2009) or by including an empirical soil moisture dependent function for g_m (Keenan et al., 2010). Given that so far no consensus exists, more

TABLE 1 | List of model variables and their definitions and units.

| Variable | Definition | Unit |
|---------------------|---|---|
| A_c | Rubisco carboxylation-limited net photosynthetic rate | $\mu\text{mol CO}_2 \text{ m}^{-2} \text{ s}^{-1}$ |
| A_j | Electron transport-limited net photosynthetic rate | $\mu\text{mol CO}_2 \text{ m}^{-2} \text{ s}^{-1}$ |
| A_n | Net photosynthetic rate | $\mu\text{mol CO}_2 \text{ m}^{-2} \text{ s}^{-1}$ |
| a_1 | Ratio of C_i to C_a for vapor saturated air | – |
| b_1 | Decreasing slope of C_i/C_a ratio with the increase of VPD | kPa^{-1} |
| C_a | Ambient CO_2 level | μbar |
| C_c | CO_2 level in the chloroplast | μbar |
| C_i | Intercellular CO_2 level | μbar |
| C_i^* | C_i -based CO_2 compensation point in the absence of R_d | μbar |
| $D_{J_{\max}}$ | Deactivation energy of J_{\max} | J mol^{-1} |
| D_{g_m} | Deactivation energy of g_m | J mol^{-1} |
| E_{g_m} | Activation energy of g_m | J mol^{-1} |
| $E_{J_{\max}}$ | Activation energy of J_{\max} | J mol^{-1} |
| $E_{K_{mC}}$ | Activation energy of K_{mC} | J mol^{-1} |
| $E_{K_{mO}}$ | Activation energy of K_{mO} | J mol^{-1} |
| E_{R_d} | Activation energy of R_d | J mol^{-1} |
| $E_{V_{c\max}}$ | Activation energy of $V_{c\max}$ | J mol^{-1} |
| f_{cyc} | Fraction of electrons at PSI following the cyclic transport around PSI | – |
| f_{pseudo} | Fraction of electrons at PSI following the pseudocyclic transport | – |
| F_m' | Maximum fluorescence | – |
| F_s | Steady-state fluorescence | – |
| g_m | Mesophyll conductance | $\text{mol m}^{-2} \text{ s}^{-1} \text{ bar}^{-1}$ |
| g_{m25} | Value of g_m when leaf temperature is 25°C | $\text{mol m}^{-2} \text{ s}^{-1} \text{ bar}^{-1}$ |
| g_s | Stomatal conductance for CO_2 diffusion | $\text{mol m}^{-2} \text{ s}^{-1}$ |
| g_0 | Residual stomatal conductance when the irradiance approaches to zero | $\text{mol m}^{-2} \text{ s}^{-1}$ |
| I_{inc} | Incident irradiance | $\mu\text{mol photon m}^{-2} \text{ s}^{-1}$ |
| J | PSII electron transport rate that is used for CO_2 fixation and photorespiration | $\mu\text{mol e}^- \text{ m}^{-2} \text{ s}^{-1}$ |
| J_{\max} | Maximum value of J under saturating irradiance | $\mu\text{mol e}^- \text{ m}^{-2} \text{ s}^{-1}$ |
| $J_{\max25}$ | Value of J_{\max} when leaf temperature is 25°C | $\mu\text{mol e}^- \text{ m}^{-2} \text{ s}^{-1}$ |
| K_{mC} | Michaelis-Menten coefficients of Rubisco for CO_2 | μbar |
| K_{mC25} | Value of K_{mC} when leaf temperature is 25°C | μbar |
| K_{mO} | Michaelis-Menten coefficients of Rubisco for O_2 | mbar |
| K_{mO25} | Value of K_{mO} when leaf temperature is 25°C | mbar |
| LMA | Leaf mass per area | g m^{-2} |
| N_a | Leaf nitrogen content per unit leaf area | $\text{g N m}^{-2} \text{ leaf}$ |
| N_b | Base leaf nitrogen content at or below which A_n is zero | $\text{g N m}^{-2} \text{ leaf}$ |
| O | Partial pressures of O_2 in the chloroplast | mbar |
| R | Universal gas constant ($=8.314$) | $\text{J K}^{-1} \text{ mol}^{-1}$ |
| R_d | Mitochondrial day respiration | $\mu\text{mol CO}_2 \text{ m}^{-2} \text{ s}^{-1}$ |
| R_{d25} | Value of R_d when leaf temperature is 25°C | $\mu\text{mol CO}_2 \text{ m}^{-2} \text{ s}^{-1}$ |
| s | Factor used to calculate electron transport rate from chlorophyll fluorescence | – |
| $S_{J_{\max}}$ | Entropy term of J_{\max} | $\text{J K}^{-1} \text{ mol}^{-1}$ |
| S_{g_m} | Entropy term of g_m | $\text{J K}^{-1} \text{ mol}^{-1}$ |
| T | Leaf temperature | $^\circ\text{C}$ |
| $V_{c\max}$ | Maximum Rubisco carboxylation rate | $\mu\text{mol CO}_2 \text{ m}^{-2} \text{ s}^{-1}$ |
| $V_{c\max25}$ | Value of $V_{c\max}$ when leaf temperature is 25°C | $\mu\text{mol CO}_2 \text{ m}^{-2} \text{ s}^{-1}$ |
| VPD | Vapor pressure deficit | kPa |
| χ_J | Slope of the linear relationship between $J_{\max25}$ and N_a | $\mu\text{mol e}^- (\text{g N})^{-1} \text{ s}^{-1}$ |
| χ_V | Slope of the linear relationship between $V_{c\max25}$ and N_a | $\mu\text{mol CO}_2 (\text{g N})^{-1} \text{ s}^{-1}$ |
| ϕ_2 | Apparent operating efficiency of PSII photochemistry | $\text{mol e}^- (\text{mol photon})^{-1}$ |
| Γ^* | CO_2 compensation point in the absence of R_d | μbar |
| κ_{2LL} | Conversion efficiency of incident light into J at strictly limiting light | $\text{mol e}^- (\text{mol photon})^{-1}$ |
| θ | Convexity factor for response of J to I_{inc} | – |
| β | Absorptance of light by leaf photosynthetic pigments | – |
| ρ_2 | Proportion of absorbed light partitioned to PSII | – |

PSI, photosystem I; PSII, photosystem II.

investigations are needed to incorporate the responses of g_m to water and nitrogen variations into the photosynthesis model.

When applying the combined FvCB, g_s and g_m model for predicting photosynthetic responses to fluctuating environmental variables, inevitably many parameters need to be quantified. Information about which parameters are conservative and which are variable depending on the treatment is extremely useful for predicting photosynthesis under diverse environmental conditions. Given the previous experience that the FvCB model parameters, once expressed as a function of N_a , are not altered by environmental variables such as elevated $[CO_2]$ (Yin, 2013), we are particularly interested in examining whether the responses of FvCB, g_s and g_m model parameters to water and nitrogen stress can be modeled using a single set of parameters when they are related to leaf nitrogen content. The objectives of this study are (i) to test whether or not water and nitrogen stress combinations change the linear relationships between photosynthetic biochemical parameters and leaf nitrogen content, and (ii) to investigate the responses of stomatal conductance model parameters and mesophyll conductance to different water and nitrogen conditions and to quantify these responses for the purpose of model simplicity. To this end, we used *Lilium* (*L. auratum* × *speciosum* “Sorbonne”) as the test plant, as this plant is commonly grown under low-investment greenhouses where plants are frequently subject to different water and nitrogen regimes.

MATERIALS AND METHODS

Plant Materials and Experimental Design

Four experiments with the same type of water and nitrogen treatments were conducted in different growth seasons in a plastic greenhouse located at Nanjing, China (32°N, 118°E) during 2009 to 2011 (Table 2). The greenhouse, covered by anti-drop polyvinyl chloride film, was composed of two spans and east-west oriented with a length of 28 m, span width of 8 m, gutter height of 3 m and arch height of 5 m. Heating pipes were installed during winter season. During summer season, the greenhouse was cooled through natural ventilation and an inner shading screen installed at the position with a distance of 1.0–1.4 m to the top. Temperature, VPD and photosynthetically active radiation are shown in the Supplementary Data (Figures S1–S3). No CO_2 enrichment was applied, and standard cultivation practices for disease and pest control were used as is common for commercial *Lilium* production in China. *Lilium* bulbs, with a circumference of 14–16 cm, were planted in plastic pots filled with substrates of sand, turf and soil (3:1:1). The physicochemical properties of the substrate are shown in Table 2. The pots, with a depth of 14 cm, upper diameter of 18 cm and bottom diameter of 12 cm, were put on seedling beds ($l \times w \times h = 25.0 \text{ m} \times 1.7 \text{ m} \times 1.0 \text{ m}$) and arranged at a density of 36 plants m^{-2} .

Two water levels were used: well-watered conditions, with a soil water potential (SWP) of -4 to -15 kPa according to Li et al. (2012), and water-deficit conditions, with a SWP of -20 to -40 kPa. The SWP at 0.1 m below the soil surface was monitored using tensiometers (SWP-100, Institute of Soil Science, Chinese Academy of Sciences) with three replicates per water level. When

the SWP reached its designed lower limit value, plants were irrigated until it reached the designed upper limit value. The SWP at 0.1 m below the soil surface and the corresponding gravimetric soil water content were measured to establish calibration curves. These curves were then used to determine the amount of water required for irrigation. The dates of starting water treatment in the four experiments are shown in Table 2.

At each water level, there were four levels of nitrogen supply: 25, 45, 65, and 85 mg available nitrogen per kg substrate (hereafter N25, N45, N65, and N85, respectively). Nitrogen was added in the substrate as urea taking into account that urea can be converted into nitrate within 1 or 2 days (Harper, 1984). The amount of urea needed was calculated based on the targeted treatment level and the amount of available nitrogen in the substrate (Table 2), and urea was directly spread in the substrate, with the dates shown in Table 2. According to Sun (2013), 65 mg available nitrogen per kg substrate is the optimal level of nitrogen supply in commercial *Lilium* production for the cultivar used in this study. Treatments, with a plot area of $2.0 \times 1.5 \text{ m}^2$ and three replicates per treatment, were arranged in a split-plot design with water level assigned to the main plots and nitrogen level to the sub-plots.

Gas Exchange and Chlorophyll Fluorescence Measurements

Gas exchange was measured on newly fully expanded leaf (the 4th leaf counting from the top downward) at flower bud visible stage using the LI-6400 Portable Photosynthesis System (Li-Cor BioScience, Lincoln, NE, USA) under 21% O_2 . In Experiment 1, both light response curves and C_i response curves were measured in order to identify any differences in photosynthesis parameter estimation by using these two types of curves. For light response curves, incident irradiance (I_{inc}) in the leaf cuvette was decreased in the series of 1,500, 1,200, 1,000, 600, 400, 200, 100, 50, 20, and $0 \mu\text{mol m}^{-2} \text{ s}^{-1}$, while keeping C_a at $370 \mu\text{mol mol}^{-1}$. For C_i response curves, C_a was increased stepwise: 50, 100, 150, 200, 250, 380, 650, 1,000, and 1,500, while keeping I_{inc} at $800 \mu\text{mol m}^{-2} \text{ s}^{-1}$. The microclimate conditions in the leaf chamber were automatically controlled. The CO_2 concentration and water vapor between leaf and the reference chamber were automatically matched before data were recorded. We found that photosynthesis parameters estimated from A_n-I_{inc} curves and A_n-C_i curves were similar (see Results). Therefore, in Experiments 2–4, only A_n-I_{inc} curves were measured, as measurement of A_n-C_i curves inevitably involves the problem of CO_2 leakage into and out of the leaf cuvette, which would require additional measurements to correct for.

Chlorophyll fluorescence was simultaneously measured using FMS2 (Hansatech Instruments Ltd, UK) at a similar position on the leaf where gas exchange was measured. The steady-state fluorescence (F_s) was measured under natural radiation level (ranged from 0 to $1,200 \mu\text{mol m}^{-2} \text{ s}^{-1}$) and saturating I_{inc} (at $1,500 \mu\text{mol m}^{-2} \text{ s}^{-1}$) after 3–5 min light adaptation, followed by applying a light pulse $> 7,000 \mu\text{mol m}^{-2} \text{ s}^{-1}$ for < 1 s to measure maximum fluorescence F'_m . The apparent operating efficiency of

TABLE 2 | Detailed information of experimental treatment conditions, physicochemical properties of the growth substrate and measurements.

| | Exp. 1 ^a | Exp. 2 ^b | Exp. 3 ^b | Exp. 4 ^b |
|---|---------------------|---------------------|---------------------|---------------------|
| EXPERIMENTAL TREATMENT CONDITIONS | | | | |
| Planting date (dd-mm-yyyy) | 27-09-2009 | 29-11-2009 | 09-09-2010 | 05-12-2010 |
| Date of starting water treatment (dd-mm-yyyy) | 20-10-2009 | 25-12-2009 | 20-10-2010 | 15-02-2011 |
| Date of starting nitrogen treatment (dd-mm-yyyy) | 18-10-2009 | 12-01-2010 | 21-10-2010 | 09-02-2011 |
| Harvesting date (dd-mm-yyyy) | 22-01-2010 | 25-04-2010 | 02-01-2011 | 02-05-2011 |
| PHYSICOCHEMICAL PROPERTIES OF THE GROWTH SUBSTRATE | | | | |
| Total N (%) | 0.03 | 0.03 | 0.02 | 0.02 |
| Organic C (%) | 2.08 | 2.08 | 2.24 | 2.24 |
| Available N (mg kg ⁻¹) | 10.10 | 10.10 | 9.67 | 9.67 |
| Available P (mg kg ⁻¹) | 15.75 | 15.75 | 11.42 | 11.42 |
| Available K (mg kg ⁻¹) | 36.97 | 36.97 | 40.38 | 40.38 |
| Bulk density (g cm ⁻³) | 1.08 | 1.08 | 1.12 | 1.12 |
| EC (mS cm ⁻¹) | 0.18 | 0.18 | 0.20 | 0.20 |
| pH | 6.22 | 6.22 | 6.01 | 6.01 |

^aIn Exp. 1, light response curve, CO₂ response curve and chlorophyll fluorescence were measured, and the combined measurement of photosynthesis and chlorophyll fluorescence under non-photorespiratory conditions was conducted.

^bIn Exps. 2–4, light response curve and chlorophyll fluorescence were measured.

photosystem II photochemistry (Φ_2) was calculated as $\Phi_2 = 1 - F_s/F_m'$ (Genty et al., 1989).

Due to inadequate environmental control in the low-investment greenhouse, air temperature and VPD hardly stayed constant although they were kept within the range suitable for *Lilium* growth (Figures S1, S2). Therefore, all gas exchange and chlorophyll fluorescence measurements in the four experiments were subjected to variations of temperature and VPD.

In order to convert chlorophyll fluorescence data on Φ_2 into electron transport rate, combined measurement of gas exchange and chlorophyll fluorescence was conducted using the LI-6400XT Portable Photosynthesis System (Li-Cor BioScience, Lincoln, NE, USA) at low oxygen using a gas blend of 2% O₂ and 98% N₂ in the leaf chamber at flower bud visible stage (Experiment 1). $A_n - I_{inc}$ curves were measured while keeping C_a at 1,000 $\mu\text{mol mol}^{-1}$, to create non-photorespiratory conditions. A_n at high C_a levels (i.e., 650, 1,000, and 1,500 $\mu\text{mol mol}^{-1}$) at 2% O₂ was also measured while keeping I_{inc} at 800 $\mu\text{mol m}^{-2} \text{s}^{-1}$. Φ_2 was assessed using the same procedure as described above. In order to establish the correlation of estimating R_d using different methods, combined measurement of gas exchange and chlorophyll fluorescence for $A_n - I_{inc}$ curves (under 21% O₂, keeping C_a at 370 $\mu\text{mol mol}^{-1}$) was also conducted in Experiment 1. All gas exchange data wherever the set-point C_a differed from the ambient CO₂ level were corrected for CO₂ leakage from measurements using thermally killed leaves.

Leaf Characteristics

After gas exchange and chlorophyll fluorescence measurements, the leaves were cut, and leaf area was measured before being put in the oven at 105°C for 30 min and subsequently at 80°C until constant weight. Leaf nitrogen concentration (for organic nitrogen) was measured by using the Kjeldahl digestion method (Sun, 2013). Briefly, leaf dry samples were ground, and a 0.5 g

of ground sample was digested with 30% hydrogen peroxide and 5 mL of concentrated sulphuric acid at 340°C. 10 mL of 10 mol L⁻¹ sodium hydroxide was then added for distilling the digested solution. The distillate was titrated using 0.02 mol L⁻¹ sulfuric acid, and bromocresol green-methyl red was used as the indicator. Leaf nitrogen content per unit leaf area (N_a , g m⁻²) was calculated based on leaf nitrogen concentration, leaf dry weight and leaf area.

Estimation of Photosynthetic Model Parameters

The FvCB model (Farquhar et al., 1980) predicts net photosynthetic rate (A_n) as the minimum of the Rubisco carboxylation-limited rate (A_c) and the electron transport-limited rate (A_j):

$$A_n = \min(A_c, A_j) \quad (1)$$

$$A_c = \frac{(C_c - \Gamma^*) V_{cmax}}{C_c + K_{mC} (1 + O/K_{mO})} - R_d \quad (2)$$

$$A_j = \frac{(C_c - \Gamma^*) J}{4C_c + 8\Gamma^*} - R_d \quad (3)$$

where C_c and O are the chloroplast partial pressures of CO₂ and O₂, respectively; K_{mC} and K_{mO} are the Michaelis-Menten coefficients of Rubisco for CO₂ and O₂, respectively; R_d is day respiration; Γ^* is the CO₂ compensation point in the absence of R_d and was calculated as $0.5 O \frac{K_{mC}}{K_{mO}} [\exp(-3.3801 + \frac{5.220}{298R(T+273)})]$ (Yin et al., 2004), derived from the parameter values of Bernacchi et al. (2001); J is the photosystem II electron transport rate that is used for CO₂ fixation and photorespiration.

R_d was firstly estimated as the y -axis intercepts of the linear regression plots of A_n against I_{inc} (the Kok method hereafter) (Sharp et al., 1984). The Kok method tends to underestimate R_d (Sharp et al., 1984; Yin et al., 2011). Therefore, R_d was also

estimated from the linear regression of A_n against $(I_{inc}\Phi_2/4)$ (the Yin method hereafter) (Yin et al., 2009, 2011) using data available from the combined measurement of gas exchange and chlorophyll fluorescence, in order to establish the calibration relationship between values of R_d estimated by the two methods. As combined gas exchange and chlorophyll fluorescence data were used only in part of our measurements, all the R_d estimated based on the Kok method was then corrected according to the established calibration relationship to obtain R_d estimates for all treatments.

The calculation of A_c or A_j in the FvCB model requires C_c , which is unknown beforehand. Therefore, A_j relevant parameters were estimated based on Yin et al. (2009) using chlorophyll fluorescence data. To convert fluorescence-based data on Φ_2 into electron transport rate J , a calibration needs to be made for each water and nitrogen treatment. This was done by linear regression plot of A_j against $(I_{inc}\Phi_2/4)$, using data obtained under non-photorespiratory conditions from low light levels of the A_n-I_{inc} curve and three high CO_2 levels. The slope s of this linear regression was used as a calibration factor to calculate values of electron transport rate under all conditions: $J = sI_{inc}\Phi_2$ (Yin et al., 2009). The obtained J was then fitted to the following equation to obtain electron transport parameters of the FvCB model:

$$J = \frac{\kappa_{2LL}I_{inc} + J_{max} - \sqrt{(\kappa_{2LL}I_{inc} + J_{max})^2 - 4\theta J_{max}\kappa_{2LL}I_{inc}}}{2\theta} \quad (4)$$

where κ_{2LL} is the conversion efficiency of incident light into J at strictly limiting light; J_{max} is the asymptotic maximum value of J when I_{inc} approaches to saturating level; θ is a convexity factor for response of J to I_{inc} , and was assumed to have a constant value of 0.8 (Yin and Struik, 2015). Since chlorophyll fluorescence measurement was conducted under fluctuating temperature, the value of J_{max} at 25 °C (J_{max25}) and κ_{2LL} were calculated by combining Equation (4) with Equation (7) (see later) that describes the temperature response of J_{max} .

With J_{max25} and κ_{2LL} calculated as described above, J_{max} for each A_n-I_{inc} curve from gas exchange measurement was derived according to the temperature level during each measurement using Equation (7) (see later). J at each light level in the A_n-I_{inc} curve was then derived using Equation (4) based on J_{max} and κ_{2LL} calculated before.

With J and R_d calculated, g_m was then estimated assuming that g_m was constant across the entire light response curve. Whether or not g_m is constant across light or CO_2 levels remains debatable, but this assumption allows the identification of any differences among water and nitrogen treatments in the actual average g_m . For that purpose, a relatively less measurement error-sensitive method, the NRH-A method (Yin and Struik, 2009a), was used to estimate the value of g_m as constant, by fitting the following non-rectangular hyperbolic (NRH) equation for the A_j part of the C_i -based FvCB model:

$$A = 0.5 \left\{ x_1 - R_d + g_m (C_i + x_2) - \sqrt{4g_m [(C_i - \Gamma^*)x_1 - R_d (C_i + x_2)]} \right\} \quad (5)$$

where $x_1 = J/4$ and $x_2 = 2\Gamma^*$; C_i is the intercellular CO_2 level. According to our experimental data, A_j -limitation in a light response curve of *Lilium* usually occurred at or below 1,000 $\mu\text{mol m}^{-2} \text{s}^{-1}$, as a good linear relationship between A_n and J was observed within this range (Figure S4). The advantages of the NRH-A method over other existing methods including the most widely used variable- J method in deriving the average g_m was fully illustrated by Yin and Struik (2009a).

Equation (5) can also be applied to calculate A_c by setting: $x_1 = V_{cmax}$ and $x_2 = K_{mC} (1 + O/K_{mO})$. V_{cmax} was then estimated by fitting the combined Eqs. (1), (4) and (5) to the entire light response curve or C_i response curve using the already estimated values of J_{max} , κ_{2LL} , R_d and g_m as input.

Temperature Responses of Photosynthesis Parameters

To account for the effect of the varying temperature during measurement, temperature response functions were introduced so that the estimation of key parameters could be adjusted to the same reference temperature for the comparison among treatments. The temperature responses of R_d and Rubisco kinetic properties (V_{cmax} , κ_{mC} and κ_{mO}) were described by an Arrhenius function Equation (6), and the temperature responses of J_{max} and g_m were described by a peaked Arrhenius function Equation (7), normalized with respect to their values at 25 °C:

$$X = X_{25}e^{(T-25)E_x/[298R(T+273)]} \quad (6)$$

$$X = X_{25}e^{(T-25)E_x/[298R(T+273)]} \left[\frac{1 + e^{(298S_x - D_x)/(298R)}}{1 + e^{(T+273)S_x - D_x/[R(T+273)]}} \right] \quad (7)$$

where X stands for each parameter; X_{25} is the value of each parameter at 25 °C (R_{d25} , V_{cmax25} , κ_{mC25} , κ_{mO25} , J_{max25} , and g_{m25}); E_x is the activation energy of each parameter (E_{Rd} , E_{Vcmax} , E_{KmC} , E_{KmO} , E_{Jmax} , and E_{gm}); S_x and D_x are the entropy term and the deactivation energy, respectively (applying to J_{max} and g_m); T is the leaf temperature; R is the universal gas constant. Since Rubisco kinetic properties are generally assumed conserved among C_3 species (von Caemmerer et al., 2009), values of κ_{mC25} , κ_{mO25} , E_{KmC} , and E_{KmO} were fixed at 272.4 μbar , 165.8 mbar, 80,990 J mol^{-1} , and 23,720 J mol^{-1} , respectively, according to Bernacchi et al. (2002). To avoid over-parameterization, E_{Rd} was fixed at 46,390 J mol^{-1} (Bernacchi et al., 2001); S_{Jmax} and D_{Jmax} were fixed at 650 $\text{J K}^{-1} \text{mol}^{-1}$ (Harley et al., 1992) and 200,000 J mol^{-1} (Medlyn et al., 2002), respectively; E_{gm} , S_{gm} , and D_{gm} were fixed at 49,600 J mol^{-1} , 1,400 $\text{J K}^{-1} \text{mol}^{-1}$, and 437,400 J mol^{-1} , respectively (Bernacchi et al., 2002).

The Relationships between Biochemical Parameters and Leaf Nitrogen Content

The photosynthetic capacity parameters V_{cmax25} and J_{max25} are linearly related to N_a (Harley et al., 1992; Braune et al., 2009):

$$V_{cmax25} = \chi_V (N_a - N_b) \quad (8)$$

$$J_{max25} = \chi_J (N_a - N_b) \quad (9)$$

where N_b is the base leaf nitrogen content at or below which A_n is zero, and a value of 0.35 $\text{g N (m}^2 \text{ leaf)}^{-1}$ was used in this study

(Archontoulis et al., 2012); χ_V is the slope of $V_{\text{cmax}25}$ against N_a , and χ_J is the slope of $J_{\text{max}25}$ against N_a .

Parameterization of the Stomatal Conductance Model

A phenomenological model for stomatal conductance for CO_2 transfer was first described by Ball et al. (1987), revised by Leuning (1995), and further revised by Yin and Struik (2009b). Li et al. (2012) called this model the BWB-Leuning-Yin model. In the model, stomatal conductance was described by:

$$g_s = g_0 + \frac{A + R_d}{C_i - C_{i^*}} f_{\text{vpd}} \quad (10)$$

where g_0 is the residual stomatal conductance when the irradiance approaches to zero; C_{i^*} is the C_i -based CO_2 compensation point in the absence of R_d and was calculated as $(\Gamma_* - R_d/g_m)$ using Γ_* , R_d and g_m calculated before as input; f_{vpd} is a function describing the effect of VPD, which is not yet understood sufficiently and may be described empirically as Yin and Struik (2009b):

$$f_{\text{vpd}} = \frac{1}{1/(a_1 - b_1 \text{VPD}) - 1} \quad (11)$$

where a_1 represents the ratio of C_i to C_a for vapor saturated air, and b_1 represents the decreasing slope of this ratio with increasing VPD, if g_0 approaches to zero. Because of this obvious meaning of a_1 and b_1 , we chose Equation (11), instead of the equation of Leuning (1995), for our analysis of the effect of VPD on g_s . Combining Equations (10) and (11), g_0 , a_1 and b_1 can be estimated by using the data of A_n , C_i and VPD obtained from gas exchange measurement. For that, measured stomatal conductance for water vapor transfer was divided by a factor 1.6 to convert it to g_s for CO_2 transfer that is required for Equation (10).

Statistical and Model Analyses

Using a non-linear regression with the GAUSS method in PROC NLIN of SAS (SAS Institute Inc., Cary, NC, USA), FvCB model parameters ($V_{\text{cmax}25}$, $J_{\text{max}25}$, κ_{2LL} , R_{d25} , g_{m25} , $E_{V_{\text{cmax}}}$, and $E_{J_{\text{max}}}$) and BWB-Leuning-Yin model parameters (g_0 , a_1 , and b_1) were estimated. Whether or not the treatment effect on each estimated parameter was significant was tested using an F -test. Following that, conserved parameter values across treatment classes were also estimated.

With these estimated parameters available, we aimed to test to what extent conserved parameter values could be used to predict A_n and g_s under water and nitrogen stress combinations, for the purpose of simplifying model parameterization. For such, a step-wise procedure was followed. First, we analyzed whether or not water and nitrogen stress combinations change the linear relationships between biochemical parameters and N_a , and tested to what extent conserved parameter values in the C_i -based FvCB model (Equation 5) could be used to predict A_n under different water and nitrogen conditions. Second, we tested to what extent conserved parameter values could be used in the BWB-Leuning-Yin model to predict g_s under different water and nitrogen

conditions. Third, we explored the coupled FvCB and BWB-Leuning-Yin model (for the analytical solution for this coupled model, see Yin and Struik, 2009b), which allows using C_a as input to predict A_n . We used this coupled model to assess to what extent conserved parameter values in both the FvCB model and the BWB-Leuning-Yin model could be used to predict A_n (using C_a as input) across various water and nitrogen treatment regimes.

RESULTS

Model Parameterization

Data of $A_n - I_{\text{inc}}$ curves showed that both water-deficit conditions and low nitrogen supply decreased A_n (Figure 1). The initial linear part of these curves was explored to estimate R_d . Values of R_d estimated by the Kok method were generally lower than those estimated by the Yin method (Figure 2). The linear correlation between values of R_d estimated by the two methods (Figure 2) was used to correct all R_d estimated by the Kok method.

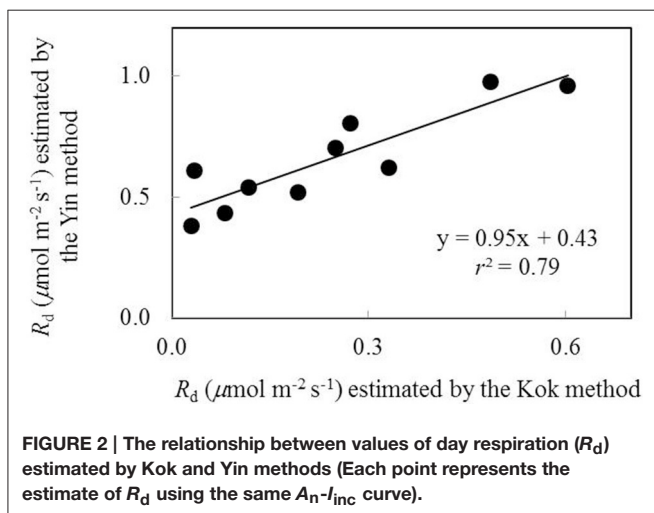
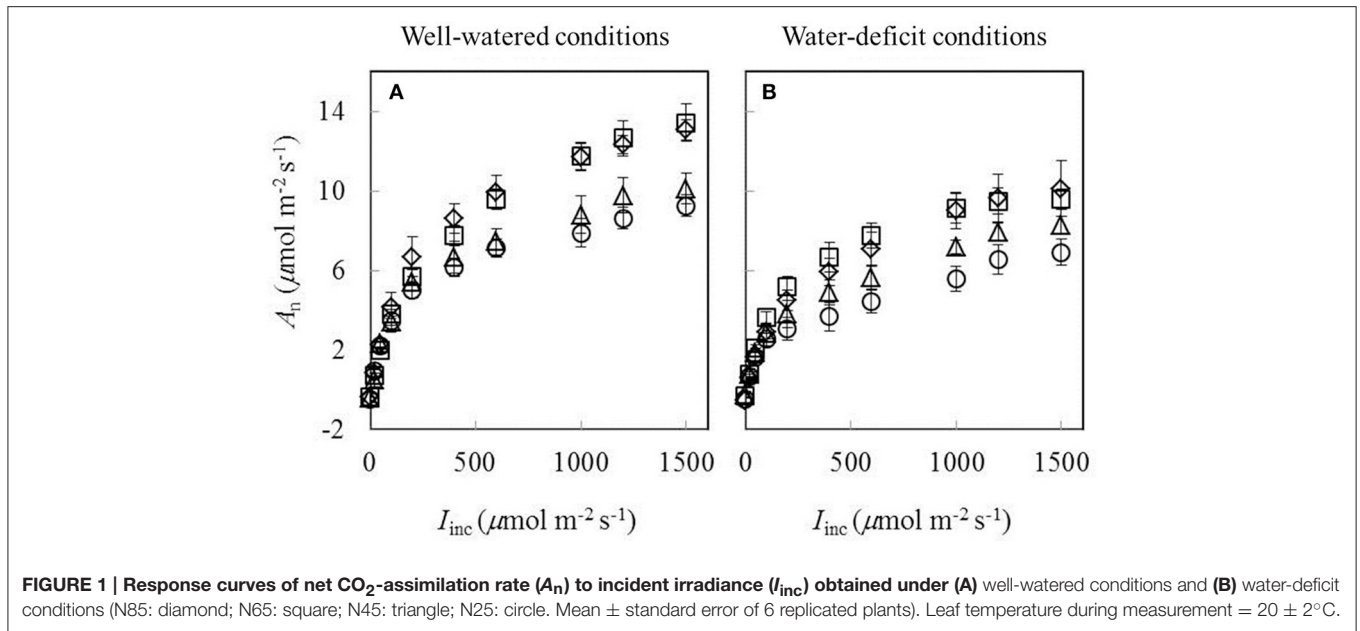
The plot of A_j against $(I_{\text{inc}} \Phi_2/4)$ using data obtained under low O_2 condition from low light levels of the $A_n - I_{\text{inc}}$ curves and three high CO_2 levels was essentially linear (Figure 3). Both water and nitrogen conditions affected the value of the linear slope s , the calibration factor used to convert Φ_2 into J . The factor decreased by low nitrogen supply and by water-deficit conditions.

V_{cmax} estimated from $A_n - I_{\text{inc}}$ curves and from available $A_n - C_i$ curves under the same measurement conditions were very similar when using the same input values of J_{max} , κ_{2LL} , R_d , and g_m (Figure 4). This suggested the reliability of using $A_n - I_{\text{inc}}$ curves to estimate V_{cmax} . The estimated parameter values of the FvCB model for each treatment are listed in Table 3, and those of the BWB-Leuning-Yin model and g_m are listed in Table 4. All parameters were reliably estimated, as the standard error values of the estimates were relatively small (Tables 3, 4).

The Response of Estimated Parameter Values to Water and Nitrogen Treatments

Water-deficit conditions significantly decreased $V_{\text{cmax}25}$, $J_{\text{max}25}$, κ_{2LL} , and R_{d25} at all nitrogen levels (Table 3). $V_{\text{cmax}25}$, $J_{\text{max}25}$, and R_{d25} decreased with decreasing of nitrogen availability whereas κ_{2LL} showed such a response to a much less clear extent under both water-deficit conditions and well-watered conditions (Table 3). $V_{\text{cmax}25}$, $J_{\text{max}25}$, and κ_{2LL} were significantly lower in the combined water deficit and low nitrogen availability treatments than in other treatments (Table 3). Neither $E_{J_{\text{max}}}$ nor $E_{V_{\text{cmax}}}$ was significantly affected by water and nitrogen treatments (Table S1).

Water-deficit conditions significantly decreased g_0 , a_1 , b_1 , and g_{m25} at all nitrogen levels (Table 4). g_0 and g_{m25} decreased with decreasing nitrogen availability whereas a_1 and b_1 responded little to nitrogen treatments under both water-deficit conditions and well-watered conditions (Table 4). g_{m25} was significantly lower under the combined water deficit and the lowest nitrogen availability treatment than in other treatments (Table 4).



The Relationships between Estimated Parameter Values and Leaf Nitrogen Content

Under both water-deficit conditions and well-watered conditions, V_{cmax25} , J_{max25} , κ_{2LL} , R_{d25} , g_{m25} , and g_0 linearly increased with increasing N_a (Figure 5). X_V and X_J were determined as $62 \mu\text{mol} (\text{g N})^{-1} \text{s}^{-1}$ and $93 \mu\text{mol} (\text{g N})^{-1} \text{s}^{-1}$, respectively (Figures 5A,C). The N_a -dependent relationship was relatively less clear for other parameters (Figures 5B,D-F), but an F -test revealed that water and nitrogen treatments did not significantly alter the linear relationships in all the six parameters. Linear relationship existed between V_{cmax25} and J_{max25} with a slope of 1.49 under different water and nitrogen treatments (Figure 6).

Comparison between Model Predictions and Measured Values for A_n and g_s

Since the linear relationships between biochemical parameters and N_a were found to exist under different treatment combinations (Figure 5), we further tested to what extent conserved parameter values could be used in the FvCB model to predict A_n under different water and nitrogen conditions. Two sets of comparisons between the measured A_n and the predicted A_n were conducted, (i) using treatment-specific parameter values (i.e., using specific parameter values obtained under each treatment) (Figures 7A,B), and (ii) using shared parameter values (i.e., incorporating the N_a -dependent linear relationships and using overall E_{Jmax} and E_{Vcmax} values) (Figures 7C,D). For this second set of comparison, the overall values of E_{Jmax} and E_{Vcmax} for all treatments were estimated (Table S1) by incorporating the linear relationships between parameters (V_{cmax25} , J_{max25} , κ_{2LL} , R_{d25} , and g_{m25}) and N_a . The coefficient of determination (r^2) between estimated and measured A_n in both comparisons ranged from 0.85 to 0.94 (Figure 7).

We also tested to what extent conserved parameter values could be used in the BWB-Leuning-Yin model (Equations 10 and 11) to predict g_s under different water and nitrogen conditions. Since nitrogen had been found to have little effect on a_1 and b_1 (Table 4) and g_0 could be linearly correlated with N_a under both well-watered conditions and water-deficit conditions (Figure 5F), we tested to what extent conserved values of a_1 , b_1 , and g_0 can be used. For this purpose, we incorporated the linear relationships between model parameters (g_0 and g_{m25}) and N_a , and estimated overall values of a_1 and b_1 for all treatments (Table 4). Three sets of comparisons between the measured g_s and the predicted g_s were conducted, (i) using treatment-specific parameter values (Figures 8A,B), (ii) using shared parameter values for each water treatment (i.e., incorporating the N_a -dependent linear relationships and

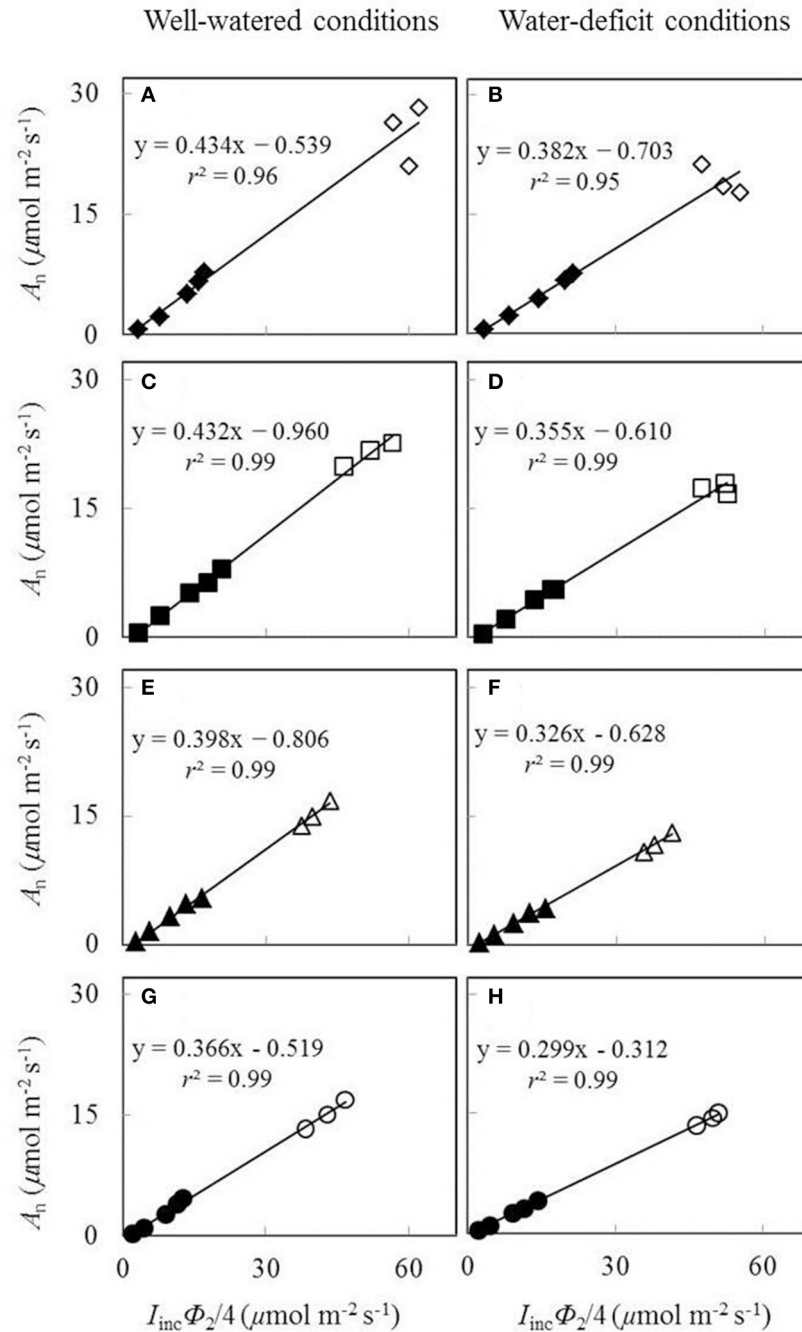
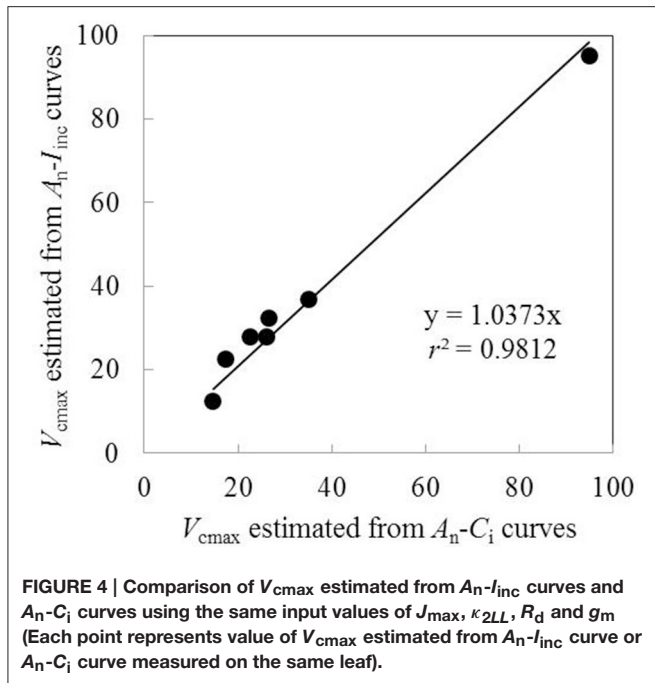


FIGURE 3 | Net CO₂-assimilation rate (A_n), measured under a non-photorespiratory condition, as a function of $I_{\text{inc}} \Phi_2/4$ under well-watered conditions (A,C,E,G) and water-deficit conditions (B,D,F,H) (N85: A,B; N65: C,D; N45: E,F; N25: G,H). Closed symbols are from low light levels of the A_n - I_{inc} curves; open symbols are from three high CO₂ levels at the same I_{inc} of $800 \mu\text{mol m}^{-2} \text{s}^{-1}$; data for open symbols and closed symbols in the same panel were measured on the same leaf; see the text).

using overall values of a_1 and b_1 for each water treatment group given in Table 4 (Figures 8C,D), and (iii) using shared parameter values for all treatments (i.e., incorporating the N_a -dependent linear relationships and using overall values of a_1 and b_1 for all treatments given Table 4) (Figures 8E,F). Using treatment-specific parameter values in the BWB-Leuning-Yin

model, the r^2 between estimated and measured g_s was 0.61 under well-watered conditions and 0.57 under a water deficit (Figures 8A,B); using shared parameter values for each water treatment, the r^2 was 0.55 for well-watered plants and 0.43 under a water deficit (Figures 8C,D). When shared parameters were used for all treatments, g_s was appreciably underestimated under



well-watered conditions (**Figure 8E**), but overestimated under a water deficit (**Figure 8F**). This third set of predictions of g_s , when compared with the first set of predictions, underestimated g_s by 9% under well-watered conditions and overestimated g_s by 13% under water-deficit conditions.

As g_s was either underestimated or overestimated by the BWB-Leuning-Yin model using shared parameter values for all treatments (**Figures 8E,F**), we further assessed the impact of this inaccurate estimation of g_s on the prediction of A_n . Two sets of comparisons between the measured A_n and the predicted A_n were conducted. In the first comparison, shared values of the FvCB model parameters for all treatments and shared values of the BWB-Leuning-Yin model parameters for each water treatment were used in the coupled model; the r^2 between estimated and measured A_n was 0.89 under well-watered conditions and 0.80 under water-deficit conditions (**Figures 9A,B**). In the second comparison, shared values of both the FvCB model parameters and the BWB-Leuning-Yin model parameters for all treatments were used; the r^2 was 0.89 under well-watered conditions (**Figure 9C**), but A_n was overestimated by 9% under water-deficit conditions (**Figure 9D**).

DISCUSSION

Methodology to Estimate Photosynthetic Parameters

In our study, all model parameters were estimated based on the A_n-I_{inc} curves, instead of A_n-C_i curves, for estimating the FvCB parameters. We tested that the estimated V_{cmax} values by using these two types of curves were quite similar (**Figure 4**), as also shown in a previous study (Archontoulis et al., 2012). The approach of using A_n-I_{inc} curves provides an alternative

to the prevailing approach of using A_n-C_i curves and has its own advantages. First, the FvCB model is commonly used to predict leaf photosynthesis in canopies under field conditions, where it is the light level, not the CO_2 level, that fluctuates most significantly in space and in time. This suggests that the FvCB parameters estimated from A_n-I_{inc} curves should more closely represent field situations, relative to those based on A_n-C_i curves. Second, using A_n-C_i curve is known to have problems of CO_2 leakage and down-regulation of Rubisco at the low level of CO_2 during the measurement. The A_n-I_{inc} curve-based approach avoids these problems since the whole response curve is measured under ambient CO_2 level. However, using A_n-I_{inc} curves also tends to have problems. First, V_{cmax} cannot always be estimated from A_n-I_{inc} curves since the entire A_n-I_{inc} curve can be A_j limited sometimes (Archontoulis et al., 2012), especially for field crops that have high light saturating point (e.g., cotton, Wise et al., 2004). Second, the rate of TPU (triose phosphate utilization), if exerting a limitation on photosynthesis, cannot be estimated using A_n-I_{inc} curves since like Rubisco limitation, any TPU limitation on A_n-I_{inc} curves also happens at high irradiance levels (Archontoulis et al., 2012). Nevertheless, our limited data (**Figure 4**) show the evidence in support of using A_n-I_{inc} curves as an alternative approach to estimate V_{cmax} . More comparisons between the two approaches using A_n-I_{inc} and using A_n-C_i curves are needed for different crop types and environments.

We adopted some parameter values from the literature as input to avoid over-parameterization of the FvCB model. First, θ (the convexity factor for response of electron transport rate to incident light) was set to a constant value of 0.8 according to Yin and Struik (2015). It is worthy to notice that the actual value of θ could vary across species and environments. In our experiment, θ may be affected by different water and nitrogen treatments, as well as different light environment caused by different growth season. Initial analyses showed that letting θ be fitted as well resulted in enormous unrealistic variation of the estimated J_{max} and κ_{2LL} . Since the biological meaning of θ is less obvious than that of J_{max} and κ_{2LL} , we decided to set θ as a constant value to avoid biased estimations of J_{max} and κ_{2LL} . Equation (4) with θ of 0.8 generates a very similar light response shape as given by the other widely used quadratic hyperbolic equation initially used by Harley et al. (1992). Second, in line with some previous studies (Xu and Baldocchi, 2003; Li et al., 2012), we adopted the activation energy of R_d (E_{Rd}) and g_m (E_{gm}), the deactivation energy of J_{max} (D_{Jmax}) and g_m (D_{gm}), and the entropy term of J_{max} (S_{Jmax}) and g_m (S_{gm}) from literature (Bernacchi et al., 2001, 2002). Whether or not these temperature response parameters change with water and nitrogen conditions is still not clear and further studies are needed. Third, Rubisco kinetic properties (κ_{mC25} , κ_{mO25} , E_{KmC} , and E_{KmO}) were adopted from Bernacchi et al. (2002). Despite the generally assumption that Rubisco kinetic properties are conserved among C_3 species (von Caemmerer et al., 2009), values of these constants reported in the literature are different (Bernacchi et al., 2001, 2002; Dreyer et al., 2001). The choice of Rubisco parameters also affected our FvCB parameter estimation. Since all parameters in the FvCB model are interrelated with each other, potential errors in our parameter estimation exist

TABLE 3 | List of parameter values (standard error of estimate in brackets if available) estimated for the FvCB model under different water and nitrogen treatments.

| Treatment | κ_{2LL} (mol mol ⁻¹) | J_{max25} (μmol m ⁻² s ⁻¹) | V_{cmax25} (μmol m ⁻² s ⁻¹) | R_{d25} (μmol m ⁻² s ⁻¹) |
|---------------------------------|---|---|--|---|
| WELL-WATERED CONDITIONS | | | | |
| N85 | 0.242 (0.017)c | 150 (6)a | 109 (8)a | 0.867 (0.18)a |
| N65 | 0.309 (0.020)a | 141 (4)b | 96 (5)b | 0.696 (0.15)abc |
| N45 | 0.238 (0.013)cd | 130 (5)c | 90 (5)b | 0.740 (0.12)ab |
| N25 | 0.251 (0.026)c | 118 (6)d | 77 (5)cd | 0.492 (0.10)cd |
| WATER-DEFICIT CONDITIONS | | | | |
| N85 | 0.218 (0.016)d | 137 (8)bc | 88 (6)bc | 0.514 (0.17)bcd |
| N65 | 0.265 (0.017)bc | 126 (3)cd | 80 (5)c | 0.448 (0.10)cd |
| N45 | 0.212 (0.029)d | 103 (7)e | 68 (4)d | 0.412 (0.16) |
| N25 | 0.172 (0.019)e | 96 (7)e | 58 (4)e | 0.409 (0.14)d |

Different letters following the data in the same column indicate significant difference ($P < 0.05$).

TABLE 4 | List of parameter values (standard error of estimate in brackets if available) estimated for parameters in the BWB-Leuning-Yin model of stomatal conductance (g_s) and for mesophyll conductance (g_m).

| Treatment | g_s | | | g_m |
|--|--|----------------|----------------------------|--|
| | g_0 (mol m ⁻² s ⁻¹) | a_1 (-) | b_1 (kPa ⁻¹) | g_{m25} (mol m ⁻² s ⁻¹ bar ⁻¹) |
| WELL-WATERED CONDITIONS | | | | |
| N85 | 0.021 (0.002)a | 0.575 (0.029)b | 0.203 (0.027)c | 0.236 (0.017)a |
| N65 | 0.019 (0.002)a | 0.671 (0.026)a | 0.275 (0.021)b | 0.197 (0.023)b |
| N45 | 0.014 (0.002)b | 0.690 (0.033)a | 0.321 (0.030)a | 0.172 (0.032)bc |
| N25 | 0.011 (0.001)cd | 0.688 (0.021)a | 0.291 (0.021)ab | 0.161 (0.035)bc |
| WATER-DEFICIT CONDITIONS | | | | |
| N85 | 0.011 (0.001)cde | 0.300 (0.041)c | 0.013 (0.025)e | 0.126 (0.014)cd |
| N65 | 0.009 (0.001)de | 0.284 (0.039)c | 0.007 (0.022)e | 0.155 (0.025)c |
| N45 | 0.008 (0.001)e | 0.308 (0.037)c | 0.023 (0.024)e | 0.103 (0.023)d |
| N25 | 0.012 (0.001)c | 0.317 (0.034)c | 0.086 (0.023)d | 0.041 (0.013)e |
| ESTIMATION OF OVERALL a_1 AND b_1 | | | | |
| Well-watered conditions | – | 0.661 (0.013) | 0.270 (0.012) | – |
| Water-deficit conditions | – | 0.262 (0.019) | 0.013 (0.012) | – |
| All treatments | – | 0.558 (0.012) | 0.197 (0.010) | – |

Different letters following the data in the same column indicate significant difference ($P < 0.05$).

if parameter values we adopted from the literature were not applicable in our study.

Photosynthetic Biochemical Parameters in Response to Water and Nitrogen Conditions

Our study showed that a long-term mild water deficit and water and nitrogen stress combinations did not have significant effects on the linear relationships between biochemical parameters of the FvCB model (i.e., J_{max25} , κ_{2LL} , V_{cmax25}) and leaf nitrogen content per unit area (N_a) (Figure 5). Previous studies showed that a short-term water deficit did not change the linear relationships between biochemical parameters and N_a (Díaz-Espejo et al., 2006; Gu et al., 2012), whereas under long-term drought, either the slopes of the relationships between biochemical parameters and N_a were changed (Wilson et al.,

2000; Díaz-Espejo et al., 2006) or considering the effect of leaf mass per area (LMA) in the linear regressions was needed (Xu and Baldocchi, 2003). A few other studies (Damour et al., 2008, 2009) found that drought totally modified the fundamental relationships between J_{max} and N_a since N_a was either increasing (Damour et al., 2008) or not affected (Damour et al., 2009) under drought whereas J_{max} decreased. The discrepancy of the response of N_a to drought found in different studies may be caused by different species. Damour et al. (2008) worked with lychee tree and Damour et al. (2009) worked with mango tree, whereas we focused on herbaceous species *Lilium* and Gu et al. (2012) worked with rice. Besides, different approaches used to estimate FvCB parameters could also affect the results in different studies. First, as stated earlier, we used A_n - I_{inc} curves to parameterize the FvCB model. Whether or not the approach of using A_n - I_{inc} curves and the approach of using A_n - C_i curves yield similar results under drought still requires

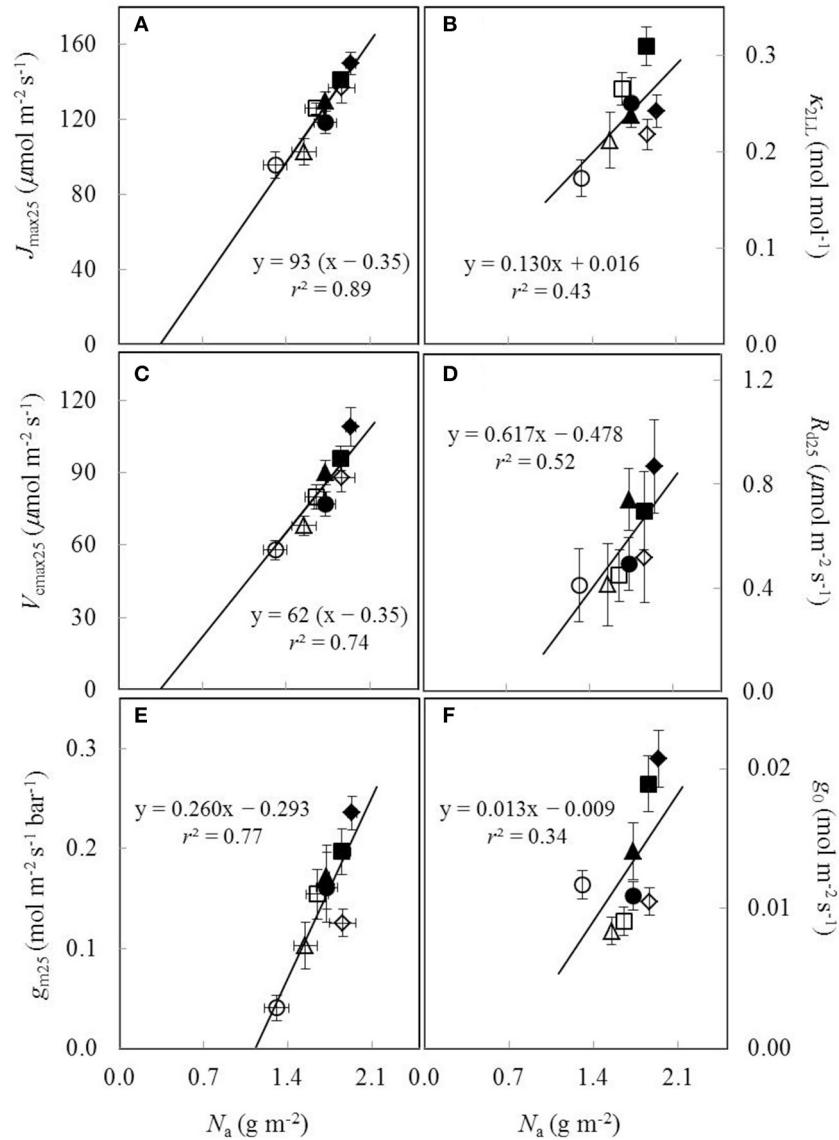
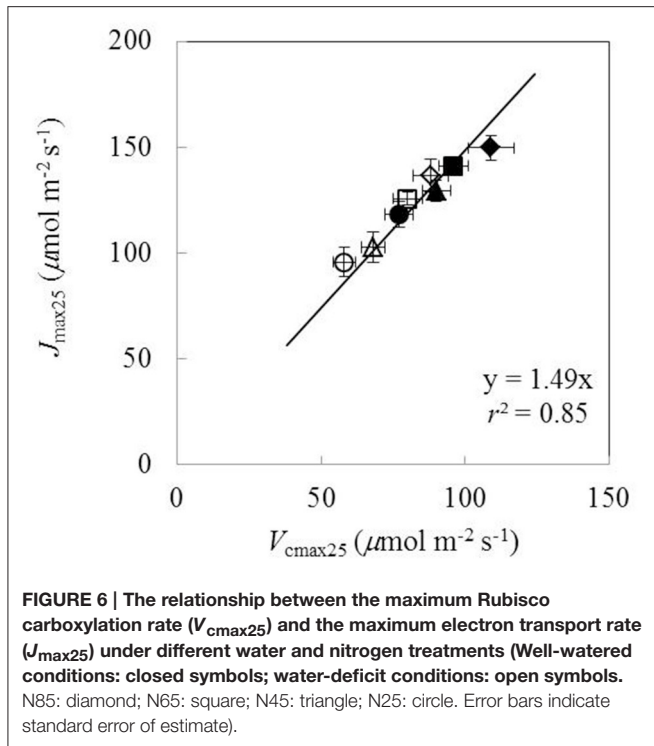


FIGURE 5 | The estimated parameters values for (A) the maximum electron transport rate ($J_{\text{max}25}$), (B) the conversion efficiency of limiting incident light into linear electron transport of photosystem II (κ_{2LL}), (C) the maximum Rubisco carboxylation rate ($V_{\text{cmax}25}$), (D) day respiration (R_{d25}), (E) mesophyll conductance (g_{m25}), and (F) residual stomatal conductance when the irradiance approaches to zero (g_0), all as a function of leaf nitrogen content (N_a) under different water and nitrogen treatments (Well-watered conditions: closed symbols; water-deficit conditions: open symbols. N85: diamond; N65: square; N45: triangle; N25: circle. Vertical error bar indicates standard error of estimate; horizontal error bar indicates standard error of the mean measured value).

more comparisons. Second, early studies tend to ignore s (the calibration factor for converting fluorescence-based efficiency of photosystem II photochemistry Φ_2 into electron transport rate J) and g_m (mesophyll conductance) during the estimation of biochemical parameters. This could lead to inaccurate estimation of biochemical parameters since both s (Figure 3) and g_m (Table 4; also reviewed in Flexas et al., 2008) decreased under drought.

The calibration factor s used to convert Φ_2 into J is actually a lumped physiological parameter ($s = \rho_2 \beta [1 - f_{\text{pseudo}} / (1 - f_{\text{cyc}})]$) that includes the absorbance of light by leaf photosynthetic

pigments (β), the proportion of absorbed light partitioned to photosystem (PS) II (ρ_2), and the fraction of electrons at PSI following the cyclic transport around PSI (f_{cyc}) and following the pseudocyclic transport (f_{pseudo}) (Yin et al., 2009; Yin and Struik, 2009a). s was found to decrease by low nitrogen supply in previous study (Yin et al., 2009), which is also found in our study (Figure 3). This decrease may be explained by the decreasing of β as a result of the decreased photosynthetic pigments in low-nitrogen leaves (Evans and Terashima, 1987). Interestingly, we found that s was smaller under water-deficit conditions compared to that under well-watered conditions despite the similar N_a



(e.g., s in N65 under well-watered conditions compared with s in N85 under water-deficit conditions). It has been reported that drought did not change the partitioning of electrons between PSI and PSII (Genty et al., 1987). However, stomatal closure caused by drought results in the decreasing of CO_2 concentration in the leaf, and consequently the amount of electrons used for CO_2 fixation decreases (Cornic and Briantais, 1991). Excessive electrons need to be consumed by other sinks apart from CO_2 fixation by following pseudo-cyclic electron transport (Cornic and Briantais, 1991; Biehler and Fock, 1996), or electrons need to follow cyclic flow around PSI (Kohzuma et al., 2009). Our results for the decreased s under water-deficit conditions independent on N_a suggest that drought induced an increase of f_{pseudo} or f_{cyc} or both in our experimental conditions.

Associated with estimating the factor s , mitochondrial day respiration (R_d) was estimated. Water-deficit conditions did not affect R_d in all N treatments, and there were non-significant effects of nitrogen on R_d under both well-watered conditions and water-deficit conditions (Table 3). Nevertheless, water-deficit conditions significantly decreased R_d in N85 and N45 treatments and generally there was a trend showing that drought and decreasing of nitrogen level decreased R_d (Table 3), as also revealed in some previous studies (González-Meler et al., 1997; Huang and Fu, 2000). Therefore, we established an N_a -dependent relationship of R_d (Figure 5F) and applied this relationship to capture the changes of R_d under different water and nitrogen conditions. The linear relationship between respiration rate and leaf nitrogen content was also found under different light conditions (Ryan, 1995) and growth locations (Reich et al., 1998).

A relatively stable J_{max25}/V_{cmax25} ratio among different water and nitrogen treatments was found in our study (Figure 6), in

line with some previous studies (Makino et al., 1992; Walcroft et al., 1997; Díaz-Espejo et al., 2006). Some studies simplified the parameterization of the FvCB model by using a fixed value for either the J_{max}/V_{cmax} ratio (Kosugi et al., 2003) or the J_{max25}/V_{cmax25} ratio (Müller et al., 2005). However, care needs to be taken in setting a constant J_{max}/V_{cmax} ratio. First, when temperature varies, this ratio cannot be constant because J_{max} and V_{cmax} have different temperature response curves. In fact, the J_{max}/V_{cmax} ratio was found to decrease with temperature increase (Walcroft et al., 1997; Medlyn et al., 2002; Díaz-Espejo et al., 2006). When scaled to a common temperature, a better correlation between J_{max} and V_{cmax} was found (Leuning, 1997). Second, g_m has a strong influence on this J_{max}/V_{cmax} ratio. In early studies (Grassi et al., 2002) when g_m was not considered, a J_{max}/V_{cmax} ratio of ca 2.0 was obtained (Leuning, 1997), which is higher than our estimate where g_m was considered (ca 1.5, Figure 6). Finally, some studies found that water and nitrogen conditions also affected the J_{max}/V_{cmax} ratio (Grassi et al., 2002; Gu et al., 2012). Therefore, the approach using a fixed value for the J_{max}/V_{cmax} ratio to parameterize the FvCB model should receive critical reservation (Xu and Baldocchi, 2003; Archontoulis et al., 2012).

In short, our study suggested that it is feasible to incorporate linear relationships between biochemical parameters and N_a in the FvCB model to predict photosynthesis under different water and nitrogen conditions, since the FvCB model using shared parameter values for all treatments gave satisfactory predictions of A_n under different water and nitrogen conditions (Figures 7C,D).

Stomatal Conductance Parameters and Mesophyll Conductance in Response to Water and Nitrogen Conditions

Accurately modeling stomatal conductance (g_s) and mesophyll conductance (g_m) are necessary steps toward predicting A_n under changing environments. The BWB-type model of g_s takes into account the effects of both environments and plant physiological status on g_s , and has been widely tested able to satisfactorily predict g_s for well-watered plants (Leuning, 1995; Li et al., 2012). Some efforts have been devoted to predict g_s under drought conditions using the BWB-type model by introducing proper approaches to adjust parameter values used in the model. In general, most studies kept g_0 (residual stomatal conductance when the irradiance approaches to zero) as a fixed value and adjusted the value for the slope (roughly represents a_1 and b_1 in the BWB-Leuning-Yin model used in our study) by introducing a modifying factor of soil moisture (Egea et al., 2011; Li et al., 2012), or precipitation and evaporation (Baldocchi, 1997), or predawn xylem water potential (Sala and Tenhunen, 1996), or leaf nitrogen content and leaf water potential (Müller et al., 2014). Leuning (1995) suggested that the BWB-type model should be able to predict g_s under water-deficit conditions by only adjusting the value for a_1 . We found that both a_1 and b_1 decreased with the decreasing of SWP (Table 4), and without considering these decreases, g_s was overestimated under water-deficit conditions (Figure 8F). Further estimation of a_1 under

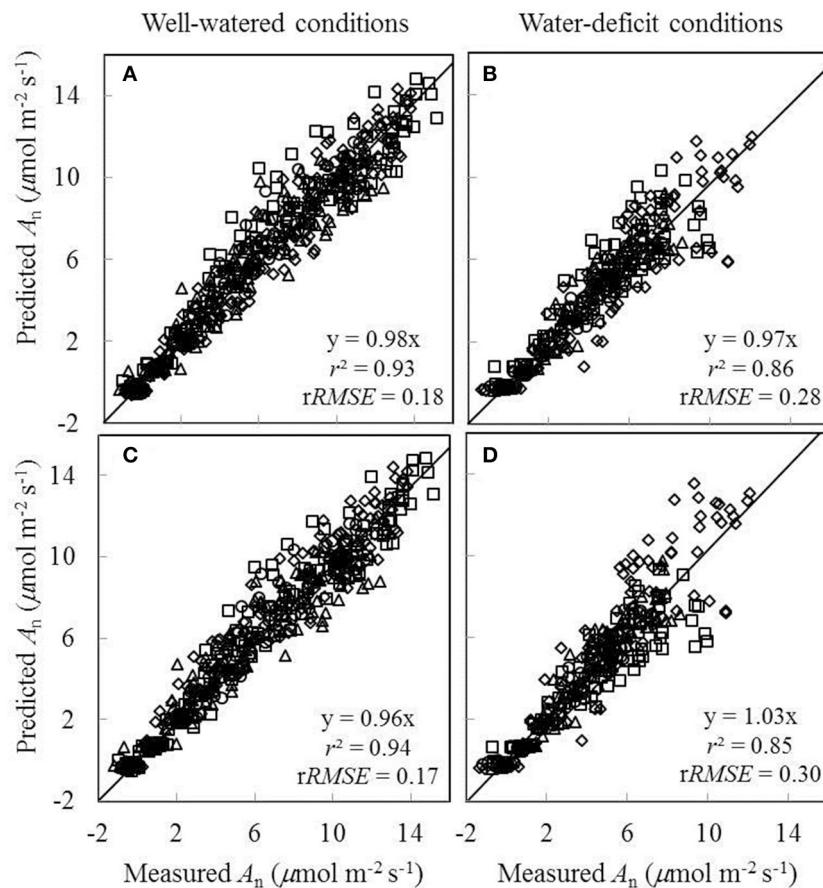


FIGURE 7 | Comparisons between the measured net CO₂-assimilation rate (A_n) and the predicted A_n by the C₁-based FvCB model either using treatment-specific parameter values (A,B), or using shared parameter values (C,D) (Well-watered conditions: A,C; water-deficit conditions: B,D). N85: diamond; N65: square; N45: triangle; N25: circle). The equation in each panel represents the linear regression of predicted (y) vs. measured values (x) by forcing the line through the origin, r^2 is the determination coefficient of the regression, and rRMSE is the relative root-mean-square error ($= \frac{1}{\bar{x}} \sqrt{\frac{\sum_{i=1}^n (y_i - x_i)^2}{n}}$, where n is the number of data points, and \bar{x} is the mean of the measured values).

water-deficit conditions by using the value for b_1 obtained under well-watered conditions resulted in a value of 0.586 for a_1 , which is much larger than the original value of 0.262 obtained under water-deficit conditions (Table 4). Therefore, values for both a_1 and b_1 need to be adjusted to properly predict g_s under water-deficit conditions. However, a_1 and b_1 were little affected by nitrogen availability (Table 4) and no correlation between a_1 and N_a , nor between b_1 and N_a , under different water and nitrogen conditions was found in our study. The approach introducing a modifying factor of leaf nitrogen content on the slope (Müller et al., 2014) is able to predict g_s in response to drought, and this could merely be due to similar responses of leaf nitrogen content and the slope to soil water condition rather than because a functional relationship exists between the slope and leaf nitrogen content. Our study did not present a quantitative relationship of a_1 and b_1 with water supply conditions since there were only two water-level treatments. Further studies including more water levels would be needed to quantify changes of a_1 and b_1 under different water and nitrogen conditions.

g_0 was affected by both water conditions and nitrogen availability (Table 4), and a linear relationship between g_0 and N_a (Figure 5F) was used in our study to take into account the changes of g_0 under different water and nitrogen conditions. Although this linear relationship is less clear compared to linear relationships between N_a and biochemical parameters (e.g., $J_{\max 25}$ and $V_{\max 25}$) (Figure 5), an F test showed that there is no significant difference between using a conserved linear relationship and using separate relationships to describe the N_a dependence of g_0 in response to water-deficit conditions. Under drought, plants tend to reserve water by reducing water loss, which makes it unlikely that g_0 is unaffected by water-deficit conditions. However, few modeling studies considered the change of g_0 under drought condition (Misson et al., 2004; Keenan et al., 2010). The reason for using a fixed value for g_0 in previous studies could be that changing the value of g_0 should not affect the prediction of g_s very much for plants with relatively high g_s since the value of g_0 itself is normally very small and approaches to zero. However, this may not hold true for plants

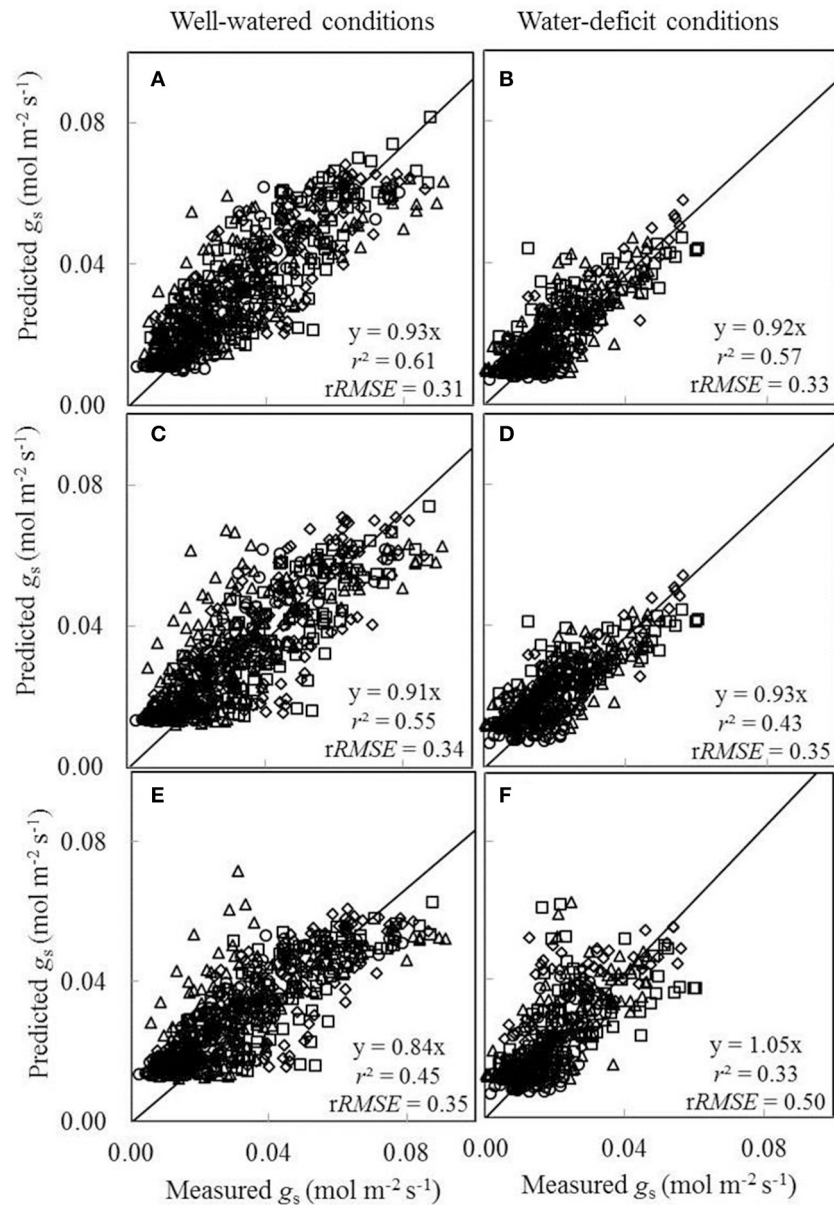


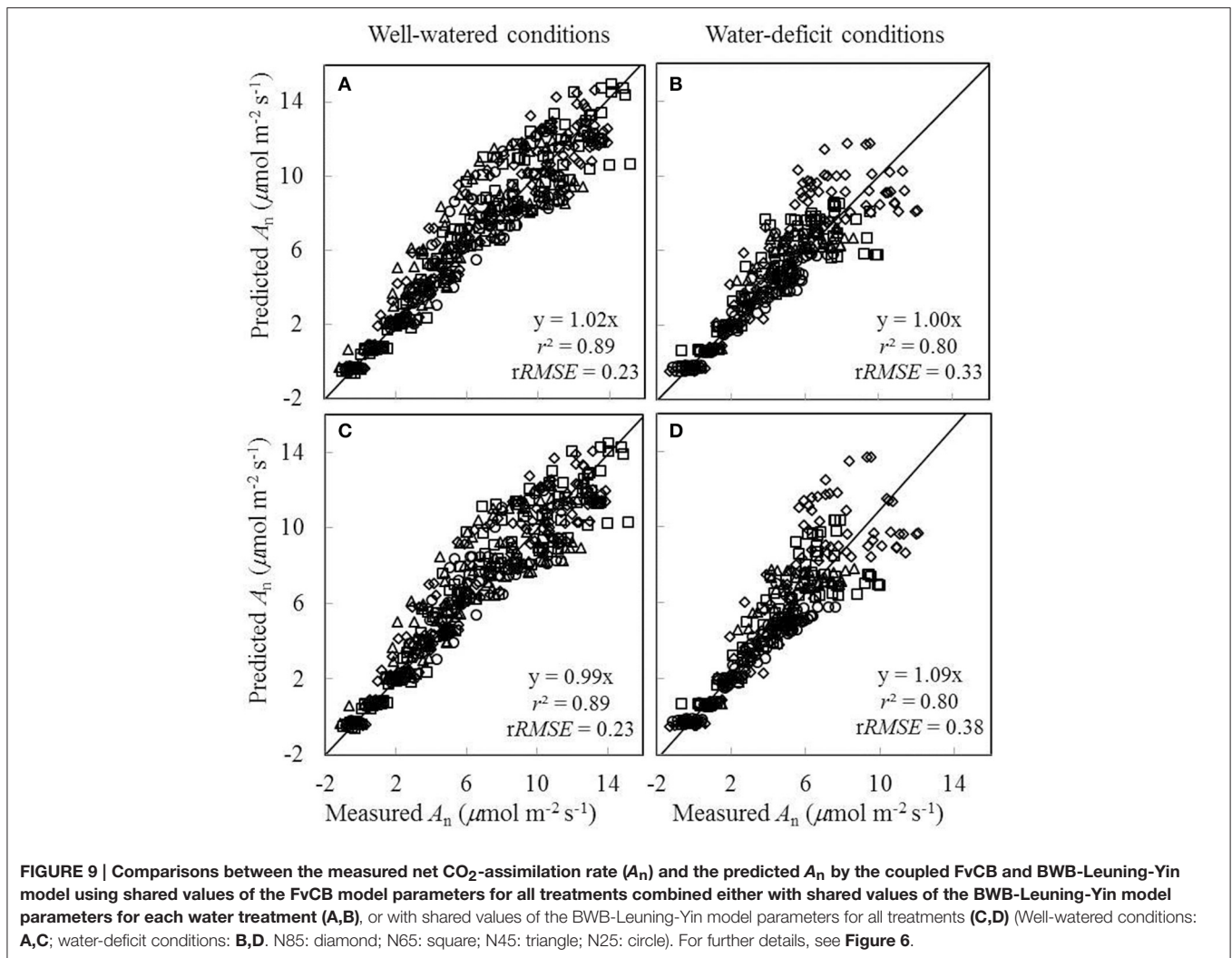
FIGURE 8 | Comparisons between the measured stomatal conductance for CO_2 diffusion (g_s) and the predicted g_s by the BWB-Leuning-Yin model either using treatment-specific parameter values (A,B), or using shared parameter values for each water treatment (C,D), or using shared parameter values for all treatments (E,F) (Well-watered conditions: A,C,E; water-deficit conditions: B,D,F. N85: diamond; N65: square; N45: triangle; N25: circle). For further details, see Figure 6.

with low g_s , as is the case in our study, since the value of g_0 may have relatively larger impact on predicting g_s .

g_m has received growing attentions in modeling photosynthesis (Niinemets et al., 2009), since g_m has been found to be finite and vary greatly among environments (Flexas et al., 2008; Yin et al., 2009). Previous studies found that g_m decreased under drought and low nitrogen availability (reviewed in Flexas et al., 2008). We found that g_m was enhanced by high nitrogen level and strongly decreased by the combination of water deficit and low nitrogen availability (Table 4). A relatively

strong linear correlation between g_m and N_a was found in our study (Figure 5E), as also found in previous studies (von Caemmerer and Evans, 1991; Warren, 2004). Such a correlation may be explained by the surface area of the chloroplasts facing the cell walls, an anatomical determinant of g_m (von Caemmerer and Evans, 1991; Evans et al., 1994), which depends on N_a .

Our results showed that the relation between g_m and N_a was hardly changed by water-deficit conditions (Figure 5E). In contrast, Gu et al. (2012) found that the change of g_m by water-deficit conditions was not explained by the change of N_a



but was negatively correlated with LMA. Nevertheless, LMA is generally considered as setting a limitation for the maximum g_m (Flexas et al., 2008; Perez-Martin et al., 2009) rather than is used to model g_m in response to environments, mainly because the change of LMA results from the long-term environmental adaptation of the plants (Poorter et al., 2009) whereas g_m can vary quickly in response to environmental changes (Flexas et al., 2006). This is supported by our result of using the N_a -dependent linear relationship to take into account the effects of water and nitrogen on g_m . Together with the incorporation of other N_a -dependent relationships of biochemical parameters, the model yielded similar results of A_n prediction compared to those using treatment-specific parameter values (Figure 7).

Some studies incorporated a dependence of g_m on g_s in the photosynthesis model (Cai et al., 2008) as a close correlation between g_s and g_m in response to soil water deficit was commonly observed (Flexas et al., 2002; Warren, 2008; Perez-Martin et al., 2009). An approach incorporating the dependence of g_m on g_s was shown to give better prediction of A_n of different genotypes than the one incorporating the dependence of g_m on leaf nitrogen (Ohsumi et al., 2007). However, the approach has been criticized

as having no physiological justification (Niinemets et al., 2009) since g_m and g_s respond differently to other environmental factors such as VPD (Warren, 2008; Perez-Martin et al., 2009). As there is not yet sufficient physiological knowledge to reliably quantify the variability of g_m , some studies merely used a modifying factor of soil water conditions to take into account the effect of water deficit on g_m (Keenan et al., 2010; Egea et al., 2011). Whether or not the linear relationship between g_m and N_a could be a promising step toward modeling the variation of g_m needs to be further tested.

The Effect of g_s Estimation on the Prediction of A_n

The coupled FvCB and BWB model has been increasingly used to model photosynthesis in response to environmental changes such as elevated CO₂ (Harley et al., 1992) and drought stress (Keenan et al., 2010; Müller et al., 2014) and seasonal changes (Kosugi et al., 2003). Normally in those previous studies, values of the biochemical parameters were related to the leaf nitrogen content and values of the stomatal conductance model parameters were changed according to the CO₂ level (Harley et al., 1992), leaf

water potential (Müller et al., 2014), or growth season (Kosugi et al., 2003).

Our study showed that considering the decreases of the stomatal conductance model parameters (a_1 and b_1) by drought was needed, otherwise, the coupled FvCB and BWB-Leuning-Yin model overestimated A_n under drought (Figure 9D) due to an overestimation of g_s (Figure 8F). The strong decrease of a_1 by drought (Table 4) indicates the decreasing of C_i/C_a ratio for vapor saturated air. The decrease of b_1 by drought (Table 4) suggests a negligible control of VPD on g_s under drought condition. These results are in line with previous studies that under drought condition, g_s at vapor nearly saturated air tended to be lower and g_s was less sensitive to VPD (Forseth and Ehleringer, 1983; Perez-Martin et al., 2009). However, an exceptional case, which g_s showed much stronger sensitivity to VPD under drought, was also found in the previous study without an explanation provided (Perez-Martin et al., 2009).

The BWB-Leuning-Yin model without considering the effect of water level on a_1 and b_1 also underestimated g_s under well-watered conditions (Figure 8E). But the subsequent prediction of A_n was not affected much (Figure 9C). This is probably explained by that under well-watered conditions, C_i is generally high and changing C_i at its high level only slightly affects A_n according to the diminishing-return relationship of A_n vs. C_i . Therefore, as shown in Figure 9, the estimation of g_s had more effect on the prediction of A_n under water-deficit conditions than under well-watered conditions.

CONCLUDING REMARKS

A previous analysis (Yin, 2013) showed that the relationship of many crop model parameters (including those FvCB biochemical parameters) as a function of plant nitrogen status was little altered by elevated CO_2 concentration. Our present study examined whether this assertion could be extended for the water and nitrogen stress combinations. We showed that the N_a dependence of biochemical parameters of the FvCB model, g_0 of the BWB-Leuning-Yin model and the g_m value were little altered by water and nitrogen stress combinations (Figure 5). By incorporating these N_a -dependent relationships with the FvCB model and BWB-Leuning-Yin model, parameterization of these models could be simplified while maintaining satisfactory predictions. The obvious exception is parameters a_1 and b_1 of the BWB-Leuning-Yin model, which depended little on nitrogen treatments but greatly on water treatments (Table 4). This is probably because the BWB-Leuning-Yin model is largely phenomenological, and its related conclusions are only valid for the specific species and conditions examined in this study. While the variation of parameters a_1 and b_1 had a great impact on the prediction of stomatal conductance, it had a considerably lower

impact on the prediction of leaf photosynthesis. Nevertheless, a further study is needed to quantify how these two parameters vary with water-deficit conditions, as they have a stronger bearing on modeling leaf transpiration.

AUTHOR CONTRIBUTIONS

NZ analyzed the data and drafted the manuscript. GL, SY, DA, and QS carried out the measurements. WL and XY made substantial contributions to conception and experimental design, and critically revised the manuscript.

ACKNOWLEDGMENTS

This research was funded by China Natural Science Foundation (31171453), and was conducted in the framework of collaboration between the College of Agriculture, Nanjing Agricultural University and the Centre for Crop Systems Analysis, Wageningen University & Research. NZ thanks the China Scholarship Council for awarding her a fellowship to conduct this work. We thank Dr. Chuang Cai for the discussion about data analysis and the two reviewers for their critical comments.

SUPPLEMENTARY MATERIAL

The Supplementary Material for this article can be found online at: <http://journal.frontiersin.org/article/10.3389/fpls.2017.00328/full#supplementary-material>

Table S1 | Activation energy of J_{max} and V_{cmax} (standard error of estimate in brackets) estimated for each water and nitrogen treatments and their shared values for all treatments. Different letters following the data in the same column indicate significant difference ($P < 0.05$).

Figure S1 | Daily mean, maximal and minimal air temperature at the height of 1.5 m above ground inside the greenhouse during (A) Exp. 1, (B) Exp. 2, (C) Exp. 3, and (D) Exp. 4. Solid curve is daily mean air temperature, dashed curve on top is the daily maximal air temperature, dotted curve at bottom is the daily minimal air temperature.

Figure S2 | Vapor pressure deficit (VPD) at the height of 1.5 m above ground inside the greenhouse during (A) Exp. 1, (B) Exp. 2, (C) Exp. 3, and (D) Exp. 4. Curve is daily mean VPD, solid line is the average daily mean VPD during the whole growth period, and dashed lines are the maximal and minimal daily mean VPD during the whole growth period, respectively.

Figure S3 | Daily mean photosynthetic active radiation (PAR) above crop canopy inside the greenhouse during (A) Exp. 1, (B) Exp. 2, (C) Exp. 3, and (D) Exp. 4. Curve is daily mean PAR, and line is the average daily mean PAR during the whole growth period.

Figure S4 | Relationships between A_n and J under well-watered conditions (A,C,E,G) and water-deficit conditions (B,D,F,H) (N85: A,B; N65: C,D; N45: E,F; N25: G,H). All data points were chosen from light levels at or below 1,000 $\mu\text{mol m}^{-2} \text{s}^{-1}$ and leaf temperature at $20 \pm 2^\circ\text{C}$ (Vertical error bar indicates standard error of measured A_n ; horizontal error bar indicates standard error of calculated J).

REFERENCES

Adam, M., Van Bussel, L. G. J., Leffelaar, P. A., Van Keulen, H., and Ewert, F. (2011). Effects of modelling detail on simulated potential crop yields

under a wide range of climatic conditions. *Ecol. Modell.* 222, 131–143. doi: 10.1016/j.ecolmodel.2010.09.001

Alton, P. B., North, P. R., and Los, S. O. (2007). The impact of diffuse sunlight on canopy light-use efficiency, gross photosynthetic product and net

- ecosystem exchange in three forest biomes. *Glob. Chang. Biol.* 13, 776–787. doi: 10.1111/j.1365-2486.2007.01316.x
- Archontoulis, S. V., Yin, X., Vos, J., Danalatos, N. G., and Struik, P. C. (2012). Leaf photosynthesis and respiration of three bioenergy crops in relation to temperature and leaf nitrogen: how conserved are biochemical model parameters among crop species? *J. Exp. Bot.* 63, 895–911. doi: 10.1093/jxb/err321
- Baldocchi, D. (1997). Measuring and modelling carbon dioxide and water vapour exchange over a temperate broad-leaved forest during the 1995 summer drought. *Plant Cell Environ.* 20, 1108–1122. doi: 10.1046/j.1365-3040.1997.d01-147.x
- Ball, J. T., Woodrow, I. E., and Berry, J. A. (1987). “A model predicting stomatal conductance and its contribution to the control of photosynthesis under different environmental conditions,” in *Progress in Photosynthesis Research*, ed J. Biggens (Dordrecht: Martinus-Nijhoff Publisher), 221–224.
- Bernacchi, C. J., Portis, A. R., Nakano, H., von Caemmerer, S., and Long, S. P. (2002). Temperature response of mesophyll conductance. Implications for the determination of rubisco enzyme kinetics and for limitations to photosynthesis in vivo. *Plant Physiol.* 130, 1992–1998. doi: 10.1104/pp.008250
- Bernacchi, C. J., Singaas, E. L., Pimentel, C., Portis, A. R. Jr., and Long, S. P. (2001). Improved temperature response functions for models of Rubisco-limited photosynthesis. *Plant Cell Environ.* 24, 253–259. doi: 10.1111/j.1365-3040.2001.00668.x
- Biehler, K., and Fock, H. (1996). Evidence for the contribution of the Mehler-peroxidase reaction in dissipating excess electrons in drought-stressed wheat. *Plant Physiol.* 112, 265–272. doi: 10.1104/pp.112.1.265
- Braune, H., Muller, J., and Diepenbrock, W. (2009). Integrating effects of leaf nitrogen, age, rank, and growth temperature into the photosynthesis-stomatal conductance model LEAFC3-N parameterised for barley (*Hordeum vulgare* L.). *Ecol. Modell.* 220, 1599–1612. doi: 10.1016/j.ecolmodel.2009.03.027
- Cai, T., Flanagan, L. B., Jassal, R. S., and Black, T. A. (2008). Modelling environmental controls on ecosystem photosynthesis and the carbon isotope composition of ecosystem-respired CO₂ in a coastal Douglas-fir forest. *Plant Cell Environ.* 31, 435–453. doi: 10.1111/j.1365-3040.2008.01773.x
- Challinor, A. J., Ewert, F., Arnold, S., Simelton, E., and Fraser, E. (2009). Crops and climate change: progress, trends, and challenges in simulating impacts and informing adaptation. *J. Exp. Bot.* 60, 2775–2789. doi: 10.1093/jxb/erp062
- Cornic, G., and Briantais, J. M. (1991). Partitioning of photosynthetic electron flow between CO₂ and O₂ reduction in a C₃ leaf (*Phaseolus vulgaris* L.) at different CO₂ concentrations and during drought stress. *Planta* 183, 178–184. doi: 10.1007/BF00197786
- Damour, G., Vandame, M., and Urban, L. (2008). Long-term drought modifies the fundamental relationships between light exposure, leaf nitrogen content and photosynthetic capacity in leaves of the lychee tree (*Litchi chinensis*). *J. Plant Physiol.* 165, 1370–1378. doi: 10.1016/j.jplph.2007.10.014
- Damour, G., Vandame, M., and Urban, L. (2009). Long-term drought results in a reversible decline in photosynthetic capacity in mango leaves, not just a decrease in stomatal conductance. *Tree Physiol.* 29, 675–684. doi: 10.1093/treephys/tpp011
- Díaz-Espejo, A., Walcroft, A. S., Fernández, J. E., Hafri, B., Palomo, M. J., and Girón, I. F. (2006). Modeling photosynthesis in olive leaves under drought conditions. *Tree Physiol.* 26, 1445–1456. doi: 10.1093/treephys/26.11.1445
- Dreyer, E., Le Roux, X., Montpied, P., Daudet, F. A., and Masson, F. (2001). Temperature response of leaf photosynthetic capacity in seedlings from seven temperate tree species. *Tree Physiol.* 21, 223–232. doi: 10.1093/treephys/21.4.223
- Egea, G., Verhoef, A., and Vidale, P. L. (2011). Towards an improved and more flexible representation of water stress in coupled photosynthesis-stomatal conductance models. *Agric. For. Meteorol.* 151, 1370–1384. doi: 10.1016/j.agrformet.2011.05.019
- Evans, J., and Terashima, I. (1987). Effects of nitrogen nutrition on electron transport components and photosynthesis in spinach. *Aust. J. Plant Physiol.* 14:59. doi: 10.1071/PP9870059
- Evans, J., von Caemmerer, S., Setchell, B., and Hudson, G. (1994). Transfer conductance and leaf anatomy in transgenic tobacco with a reduced content of rubisco. *Aust. J. Plant Physiol.* 21, 475. doi: 10.1071/PP9940475
- Farquhar, G. D., von Caemmerer, S., and Berry, J. A. (1980). A biochemical model of photosynthetic CO₂ assimilation in leaves of C₃ species. *Planta* 149, 78–90. doi: 10.1007/BF00386231
- Flexas, J., Bota, J., Escalona, J. M., Sampol, B., and Medrano, H. (2002). Effects of drought on photosynthesis in grapevines under field conditions: an evaluation of stomatal and mesophyll limitations. *Funct. Plant Biol.* 29, 461. doi: 10.1071/PP01119
- Flexas, J., Ribas-Carbó, M., Bota, J., Galmés, J., Henkle, M., Martínez-Cañellas, S., et al. (2006). Decreased Rubisco activity during water stress is not induced by decreased relative water content but related to conditions of low stomatal conductance and chloroplast CO₂ concentration. *New Phytol.* 172, 73–82. doi: 10.1111/j.1469-8137.2006.01794.x
- Flexas, J., Ribas-Carbó, M., Diaz-Espejo, A., Galmés, J., and Medrano, H. (2008). Mesophyll conductance to CO₂: current knowledge and future prospects. *Plant. Cell Environ.* 31, 602–621. doi: 10.1111/j.1365-3040.2007.01757.x
- Forseth, I. N., and Ehleringer, J. R. (1983). Ecophysiology of two solar tracking desert winter annuals. III. Gas exchange responses to light, CO₂ and VPD in relation to long-term drought. *Oecologia* 57, 344–351. doi: 10.1007/BF00377179
- Genty, B., Briantais, J. M., and Baker, N. R. (1989). The relationship between the quantum yield of photosynthetic electron transport and quenching of chlorophyll fluorescence. *Biochim. Biophys. Acta Gen. Subj.* 990, 87–92. doi: 10.1016/S0304-4165(89)80016-9
- Genty, B., Briantais, J. M., and Da Silva, J. B. (1987). Effects of drought on primary photosynthetic processes of cotton leaves. *Plant Physiol.* 83, 360–364. doi: 10.1104/pp.83.2.360
- González-Meler, M. A., Matamala, R., and Penuelas, J. (1997). Effects of prolonged drought stress and nitrogen deficiency on the respiratory O₂ uptake of bean and pepper leaves. *Photosynthetica* 34, 505–512. doi: 10.1023/A:1006801210502
- Grassi, G., Meir, P., Cromer, R., Tompkins, D., and Jarvis, P. G. (2002). Photosynthetic parameters in seedlings of *Eucalyptus grandis* as affected by rate of nitrogen supply. *Plant Cell Environ.* 25, 1677–1688. doi: 10.1046/j.1365-3040.2002.00946.x
- Gu, J., Yin, X., Stomph, T. J., Wang, H., and Struik, P. C. (2012). Physiological basis of genetic variation in leaf photosynthesis methylation and chromatin patterning among rice (*Oryza sativa* L.) introgression lines under drought and well-watered conditions. *J. Exp. Bot.* 63, 5137–5153. doi: 10.1093/jxb/ers170
- Harley, P. C., Thomas, R. B., Reynolds, J. F., and Strain, B. R. (1992). Modeling photosynthesis of cotton grown in elevated CO₂. *Plant Cell Environ.* 15, 271–282. doi: 10.1111/j.1365-3040.1992.tb00974.x
- Harper, J. (1984). “Uptake of nitrogen forms by roots and leaves,” in *Nitrogen in crop production*, ed R. Hauck (American Society of Agronomy), 165–170. Available online at: <https://dl.sciencesocieties.org/publications/books/abstracts/acesspublicati/nitrogenincropp/165>
- Hérault, A., Lin, Y. S., Bourne, A., Medlyn, B. E., and Ellsworth, D. S. (2013). Optimal stomatal conductance in relation to photosynthesis in climatically contrasting *Eucalyptus* species under drought. *Plant Cell Environ.* 36, 262–274. doi: 10.1111/j.1365-3040.2012.02570.x
- Huang, B., and Fu, J. (2000). Photosynthesis, respiration, and carbon allocation of two cool-season perennial grasses in response to surface soil drying. *Plant Soil* 227, 17–26. doi: 10.1023/A:1026512212113
- Jamieson, P. D., Porter, J. R., Goudriaan, J., Ritchie, J. T., Van Keulen, H., and Stol, W. (1998). A comparison of the models AFRCWHEAT2, CERES-Wheat, Sirius, SUCROS2 and SWHEAT with measurements from wheat grown under drought. *F. Crop. Res.* 55, 23–44. doi: 10.1016/S0378-4290(97)00060-9
- Keenan, T., Sabate, S., and Gracia, C. (2010). Soil water stress and coupled photosynthesis-conductance models: bridging the gap between conflicting reports on the relative roles of stomatal, mesophyll conductance and biochemical limitations to photosynthesis. *Agric. For. Meteorol.* 150, 443–453. doi: 10.1016/j.agrformet.2010.01.008
- Kohzuma, K., Cruz, J. A., Akashi, K., Hoshiyasu, S., Munekage, Y. N., Yokota, A., et al. (2009). The long-term responses of the photosynthetic proton circuit to drought. *Plant Cell Environ.* 32, 209–219. doi: 10.1111/j.1365-3040.2008.01912.x
- Kosugi, Y., Shibata, S., and Kobashi, S. (2003). Parameterization of the CO₂ and H₂O gas exchange of several temperate deciduous broad-leaved trees at the leaf scale considering seasonal changes. *Plant Cell Environ.* 26, 285–301. doi: 10.1046/j.1365-3040.2003.00960.x

- Leuning, R. (1995). A critical appraisal of a stomatal-photosynthesis model for C_3 plants. *Plant, Cell Environ.* 18, 339–355. doi: 10.1111/j.1365-3040.1995.tb00370.x
- Leuning, R. (1997). Scaling to a common temperature improves the correlation between the photosynthesis parameters J_{max} and V_{cmax} . *J. Exp. Bot.* 48, 345–347. doi: 10.1093/jxb/48.2.345
- Li, G., Lin, L., Dong, Y., An, D., Li, Y., Luo, W., et al. (2012). Testing two models for the estimation of leaf stomatal conductance in four greenhouse crops cucumber, chrysanthemum, tulip and lily. *Agric. For. Meteorol.* 165, 92–103. doi: 10.1016/j.agrformet.2012.06.004
- Makino, A., Sakashita, H., Hidema, J., Mae, T., Ojima, K., and Osmond, B. (1992). Distinctive responses of ribulose-1,5-bisphosphate carboxylase and carbonic anhydrase in wheat leaves to nitrogen nutrition and their possible relationships to CO_2 -transfer resistance. *Plant Physiol.* 100, 1737–1743. doi: 10.1104/pp.100.4.1737
- Maseyk, K. S., Lin, T., Rotenberg, E., Grünzweig, J. M., Schwartz, A., and Yakir, D. (2008). Physiology-phenology interactions in a productive semi-arid pine forest. *New Phytol.* 178, 603–616. doi: 10.1111/j.1469-8137.2008.02391.x
- Medlyn, B. E., Dreyer, E., Ellsworth, D., Forstreuter, M., Harley, P. C., Kirschbaum, M. U. F., et al. (2002). Temperature response of parameters of a biochemically based model of photosynthesis. II. A review of experimental data. *Plant Cell Environ.* 25, 1167–1179. doi: 10.1046/j.1365-3040.2002.00891.x
- Misson, L., Panek, J. A., and Goldstein, A. H. (2004). A comparison of three approaches to modeling leaf gas exchange in annually drought-stressed ponderosa pine forests. *Tree Physiol.* 24, 529–541. doi: 10.1093/treephys/24.5.529
- Misson, L., Rasse, D. P., Vincke, C., Aubinet, M., and François, L. (2002). Predicting transpiration from forest stands in Belgium for the 21st century. *Agric. For. Meteorol.* 111, 265–282. doi: 10.1016/S0168-1923(02)00039-4
- Monti, A. (2006). The effect of transient and continuous drought on yield, photosynthesis and carbon isotope discrimination in sugar beet (*Beta vulgaris* L.). *J. Exp. Bot.* 57, 1253–1262. doi: 10.1093/jxb/erj091
- Müller, J., Eschenröder, A., and Christen, O. (2014). LEAFC3-N photosynthesis, stomatal conductance, transpiration and energy balance model: finite mesophyll conductance, drought stress, stomata ratio, optimized solution algorithms, and code. *Ecol. Modell.* 290, 134–145. doi: 10.1016/j.ecolmodel.2013.10.036
- Müller, J., Wernecke, P., and Diepenbrock, W. (2005). LEAFC3-N: a nitrogen-sensitive extension of the CO_2 and H_2O gas exchange model LEAFC3 parameterised and tested for winter wheat (*Triticum aestivum* L.). *Ecol. Modell.* 183, 183–210. doi: 10.1016/j.ecolmodel.2004.07.025
- Niinemets, Ü., Díaz-Espejo, A., Flexas, J., Galmés, J., and Warren, C. R. (2009). Importance of mesophyll diffusion conductance in estimation of plant photosynthesis in the field. *J. Exp. Bot.* 60, 2271–2282. doi: 10.1093/jxb/erp063
- Ohsumi, A., Hamasaki, A., Nakagawa, H., Yoshida, H., Shiraiwa, T., and Horie, T. (2007). A model explaining genotypic and ontogenetic variation of leaf photosynthetic rate in rice (*Oryza sativa*) based on leaf nitrogen content and stomatal conductance. *Ann. Bot.* 99, 265–273. doi: 10.1093/aob/mcl253
- Palosuo, T., Kersebaum, K. C., Angulo, C., Hlavinka, P., Moriondo, M., Olesen, J. E., et al. (2011). Simulation of winter wheat yield and its variability in different climates of Europe: a comparison of eight crop growth models. *Eur. J. Agron.* 35, 103–114. doi: 10.1016/j.eja.2011.05.001
- Perez-Martin, A., Flexas, J., Ribas-Carbó, M., Bota, J., Tomás, M., Infante, J. M., et al. (2009). Interactive effects of soil water deficit and air vapour pressure deficit on mesophyll conductance to CO_2 in *Vitis vinifera* and *Olea europaea*. *J. Exp. Bot.* 60, 2391–2405. doi: 10.1093/jxb/erp145
- Poorter, H., Niinemets, U., Poorter, L., Wright, I. J., and Villar, R. (2009). Causes and consequences of variation in leaf mass per area (LMA): a meta-analysis. *New Phytol.* 182, 565–588. doi: 10.1111/j.1469-8137.2009.02830.x
- Qian, T., Elings, A., Dieleman, J. A., Gort, G., and Marcelis, L. F. M. (2012). Estimation of photosynthesis parameters for a modified Farquhar-von Caemmerer-Berry model using simultaneous estimation method and nonlinear mixed effects model. *Environ. Exp. Bot.* 82, 66–73. doi: 10.1016/j.envexpbot.2012.03.014
- Reich, P. B., Walters, M., Tjoelker, M., Vanderklein, D., and Buschena, C. (1998). Photosynthesis and respiration rates depend on leaf and root morphology and nitrogen concentration in nine boreal tree species differing in relative growth rate. *Funct. Ecol.* 12, 395–405. doi: 10.1046/j.1365-2435.1998.00209.x
- Ryan, M. G. (1995). Foliar maintenance respiration of sub-alpine and boreal trees and shrubs in relation to nitrogen-content. *Plant Cell Environ.* 18, 765–772. doi: 10.1111/j.1365-3040.1995.tb00579.x
- Sala, A., and Tenhunen, J. D. (1996). Simulations of canopy net photosynthesis and transpiration in *Quercus ilex* L. under the influence of seasonal drought. *Agric. For. Meteorol.* 78, 203–222. doi: 10.1016/0168-1923(95)02250-3
- Sharp, R. E., Matthews, M. A., and Boyer, J. S. (1984). Kok effect and the quantum yield of photosynthesis: light partially inhibits dark respiration. *Plant Physiol.* 75, 95–101. doi: 10.1104/pp.75.1.95
- Sun, Q. (2013). *Quantifying the Effect of Nitrogen on External Quality of Cut Lily in Greenhouse*. (in Chinese with English abstract). Available online at: <http://cdmd.cnki.com.cn/Article/CDMD-10307-1014216371.htm>
- Tuzet, A., Perrier, A., and Leuning, R. (2003). A coupled model of stomatal conductance, photosynthesis. *Plant Cell Environ.* 26, 1097–1116. doi: 10.1046/j.1365-3040.2003.01035.x
- von Caemmerer, S., and Evans, J. (1991). Determination of the average partial pressure of CO_2 in chloroplasts from leaves of several C_3 plants. *Aust. J. Plant Physiol.* 18, 287. doi: 10.1071/PP9910287
- von Caemmerer, S., Farquhar, G., and Berry, J. (2009). “Biochemical model of C_3 photosynthesis,” in *Photosynthesis in Silico: Understanding Complexity from Molecules to Ecosystems*, Vol. 29. Advances in Photosynthesis and Respiration, eds A. Laik, L. Nedbal, and Govindjee (Springer Science + Business Media B.V. Netherlands), 209–230. doi: 10.1007/978-1-4020-9237-4_9
- Walcroft, A., Whitehead, D., Silvester, W., and Kelliher, F. (1997). The response of photosynthetic model parameters to temperature and nitrogen concentration in *Pinus radiata* D. *Don. Plant, Cell Environ.* 20, 1338–1348. doi: 10.1046/j.1365-3040.1997.d01-31.x
- Wang, Y. P., and Leuning, R. (1998). A two-leaf model for canopy conductance, photosynthesis and partitioning of available energy I: model description and comparison with a multi-layered model. *Agric. For. Meteorol.* 91, 89–111. doi: 10.1016/S0168-1923(98)00061-6
- Warren, C. R. (2004). The photosynthetic limitation posed by internal conductance to CO_2 movement is increased by nutrient supply. *J. Exp. Bot.* 55, 2313–2321. doi: 10.1093/jxb/erh239
- Warren, C. R. (2008). Soil water deficits decrease the internal conductance to CO_2 transfer but atmospheric water deficits do not. *J. Exp. Bot.* 59, 327–334. doi: 10.1093/jxb/erm314
- Wilson, K. B., Baldocchi, D. D., and Hanson, P. J. (2000). Spatial and seasonal variability of photosynthetic parameters and their relationship to leaf nitrogen in a deciduous forest. *Tree Physiol.* 20, 565–578. doi: 10.1093/treephys/20.9.565
- Wise, R. R., Olson, A. J., Schrader, S. M., and Sharkey, T. D. (2004). Electron transport is the functional limitation of photosynthesis in field-grown pima cotton plants at high temperature. *Plant, Cell Environ.* 27, 717–724. doi: 10.1111/j.1365-3040.2004.01171.x
- Xu, L., and Baldocchi, D. D. (2003). Seasonal trends in photosynthetic parameters and stomatal conductance of blue oak (*Quercus douglasii*) under prolonged summer drought and high temperature. *Tree Physiol.* 23, 865–877. doi: 10.1093/treephys/23.13.865
- Yin, X. (2013). Improving ecophysiological simulation models to predict the impact of elevated atmospheric CO_2 concentration on crop productivity. *Ann. Bot.* 112, 465–475. doi: 10.1093/aob/mct016
- Yin, X., and Struik, P. C. (2009b). C_3 and C_4 photosynthesis models: an overview from the perspective of crop modelling. *NJAS Wageningen J. Life Sci.* 57, 27–38. doi: 10.1016/j.njas.2009.07.001
- Yin, X., and Struik, P. C. (2009a). Theoretical reconsiderations when estimating the mesophyll conductance to CO_2 diffusion in leaves of C_3 plants by analysis of combined gas exchange and chlorophyll fluorescence measurements. *Plant, Cell Environ.* 32, 1513–1524. doi: 10.1111/j.1365-3040.2009.02016.x
- Yin, X., and Struik, P. C. (2015). Constraints to the potential efficiency of converting solar radiation into phytoenergy in annual crops: from leaf biochemistry to canopy physiology and crop ecology. *J. Exp. Bot.* 66, 6535–6549. doi: 10.1093/jxb/erv371
- Yin, X., Struik, P. C., Romero, P., Harbinson, J., Evers, J. B., Van Der Putten, P. E. L., et al. (2009). Using combined measurements of gas exchange and chlorophyll fluorescence to estimate parameters of a biochemical C_3 photosynthesis model: a critical appraisal and a new integrated approach applied to leaves

- in a wheat (*Triticum aestivum*) canopy. *Plant Cell Environ.* 32, 448–464. doi: 10.1111/j.1365-3040.2009.01934.x
- Yin, X., Sun, Z., Struik, P. C., and Gu, J. (2011). Evaluating a new method to estimate the rate of leaf respiration in the light by analysis of combined gas exchange and chlorophyll fluorescence measurements. *J. Exp. Bot.* 62, 3489–3499. doi: 10.1093/jxb/err038
- Yin, X., Van Oijen, M., and Schapendonk, A. H. C. M. (2004). Extension of a biochemical model for the generalized stoichiometry of electron transport limited C₃ photosynthesis. *Plant. Cell Environ.* 27, 1211–1222. doi: 10.1111/j.1365-3040.2004.01224.x
- Zhou, S., Duursma, R. A., Medlyn, B. E., Kelly, J. W. G., and Prentice, I. C. (2013). How should we model plant responses to drought? An analysis of stomatal and non-stomatal responses to water stress. *Agric. For. Meteorol.* 182–183, 204–214. doi: 10.1016/j.agrformet.2013.05.009
- Zhu, G. F., Li, X., Su, Y. H., Lu, L., and Huang, C. L. (2011). Seasonal fluctuations and temperature dependence in photosynthetic parameters and stomatal conductance at the leaf scale of *Populus euphratica* Oliv. *Tree Physiol.* 31, 178–195. doi: 10.1093/treephys/tpr005
- Conflict of Interest Statement:** The authors declare that the research was conducted in the absence of any commercial or financial relationships that could be construed as a potential conflict of interest.
- The reviewer DT and handling Editor declared their shared affiliation, and the handling Editor states that the process nevertheless met the standards of a fair and objective review.
- Copyright © 2017 Zhang, Li, Yu, An, Sun, Luo and Yin. This is an open-access article distributed under the terms of the Creative Commons Attribution License (CC BY). The use, distribution or reproduction in other forums is permitted, provided the original author(s) or licensor are credited and that the original publication in this journal is cited, in accordance with accepted academic practice. No use, distribution or reproduction is permitted which does not comply with these terms.